universität wien

MASTERARBEIT / MASTER'S THESIS

Titel der Masterarbeit / Title of the Master's Thesis

„Integrated T-Cell Analysis of Adenocarcinomas of the Lung: Correlation with Clinical Data and Immune Response Markers"

verfasst von / submitted by

Mario Böhm, Bsc

angestrebter akademischer Grad / in partial fulfilment of the requirements for the degree of

Master of Science (MSc)

Wien, 2015 / Vienna 2015

Studienkennzahl lt. Studienblatt / degree programme code as it appears on the student record sheet:	A 066 830
Studienrichtung lt. Studienblatt / degree programme as it appears on the student record sheet:	Masterstudium Molekulare Mikrobiologie, Mikrobielle Ökologie und Immunbiologie UG2002
Betreut von / Supervisor:	Univ. Prof. Dr. Thomas Decker

ACKNOWLEDGEMENTS

I wish to thank, first and foremost, my supervisor Dr. Stephan-Michael Schmidbauer, who gave me the opportunity to conduct my study in his research group. Thank you for the expert support. I have learned many things since I became your student. My sincere thanks also goes to Dr. Norbert Schweifer and Dr. Tilman Voss. Without their superior knowledge and experience it would not be possible to conduct this research. I cannot find words to express my gratitude to my colleagues Nicole Budano and Oliver Bergner for their guidance, valuable comments and encouragement from the start until the end of my study. I wish to thank my colleagues and friends at Boehringer Ingelheim for sharing me numerous coffees, lunches, and funny moments. A heartfelt thanks goes out to my girlfriend Kathrin for all your love, support and patience when I was only thinking about working on my project. I am extremely fortunate to have my family, who has given me nothing but unconditional love and support throughout the past year. I also want to thank Christl and Bernd Wiletel. I am happy to have such a supportive family, standing behind me.

TABLE OF CONTENTS

ABSTRACT

Aim: Cancer remains one of the leading causes of death worldwide and after its diagnosis the therapeutic approach and prognosis is routed most commonly by classification of the UICC-TNM classification system, describing the size and invasiveness of the primary tumor and the pattern of metastases. With begin of the era of immunotherapy in oncology, it has been shown that the UICC-TNM classification alone provides limited information relating to the clinical outcome and new prognostic, and also pharmaco-dynamic markers reflecting anti-tumor immune responses are on the rise. In the current study, we analyzed the correlation of the number and distribution of tumor infiltrating CD3+ lymphocytes in tissue sections from adenocarcinomas of the lung of 29 donors with the TNM-score, gene expression analysis, plasma markers and the modified Glasgow Prognostic Score (mGPS) to assess their probable suitability as potential prognostic factor. Since the microscopical analysis of immune-stained cells is a time consuming process with intra- and inter-observer variability, a method was developped for the automated quantification of infiltrating T-cells, using the state of the art image analysis software Definiens Tissue Studio® (Definiens AG, Germany), allowing to count T-cells separately in two different tumor compartments: tumor epithelium and stroma.
Results: In the current study, we could demonstrate a correlation of T-cells infiltrating the tumor epithelium with the mRNA- expression of 40 genes involved in T-cell responses (e.g. Granzyme A/B, LAG-3, IFN-γ, ZAP70). No correlation could be observed for T-cells in tumor stroma or total tumor, also no correlation was found between T-cells in any compartment or total tumor with plasma markers or the mGPS.
Conclusion: An image analysis method was developed for the semi-automated quantitative and precise assessment of tumor infiltrating T-cells separately for tumor epithelium and stroma. T-cell densities within the tumor epithelium did correlate with 40 genes directly involved in immune responses, indicating that the tumor epithelium compared to stroma or total tumor may be a compartment with a higher potential for T-cell related biomarker research. To further elucidate the value of number and distribution of T-cells within adenocarcinomas of the lung, our results could be the trigger for additional studies, e.g. including more detailed clinical information and micro-dissected tissues samples (epithelium and stroma) for mRNA-analysis.

ZUSAMMENFASSUNG

Zielsetzung: Nach der Diagnose von Krebs, eine der häufigsten Todesursachen weltweit, werden der therapeutische Ansatz und die Prognose durch das UICC-TNM-Klassifikations System geleitet, welches die Größe und die Invasivität des Primärtumors sowie Anzeichen von möglichen Metastasen beschreibt. Mit Beginn der Ära der Immuntherapie in der Krebsforschung, hat sich gezeigt, dass die UICC-TNM-Klassifikation alleine nur begrenzte Informationen über den klinischen Ausgang bietet. Großes Interesse gilt neuen prognostischen als auch pharmakodynamische Markern die Anti-Tumor-Immunantworten reflektieren. In der aktuellen Studie untersuchten wir die Korrelation zwischen der Anzahl und Verteilung von Tumor-infiltrierenden CD3+ Lymphozyten in Gewebeschnitten von 29 Adenokarzinomen der Lunge mit dem TNM-Score, Genexpressionanalysen, Plasmamarkern und dem modifizierten Glasgow Prognostic Score (mGPS) um eine etwaige Eignung als möglichen prognostischen Faktor zu bewerten. Da die mikroskopische Analyse von immunhistochemisch dargestellten Zellen ein zeitraubender und fehleranfälliger Prozess ist, wurde hierzu eine Methode zur automatischen Quantifizierung von infiltrierenden T-Zellen mit der Bildanalyse-Software Definiens Tissue Studio® (Definiens AG, Deutschland) entwickelt, um T-Zellen in den wesentlichen beiden Tumorregionen separat zu erfassen: Tumorepithel und -stroma.
Ergebnisse: In der gegenwärtigen Studie konnte eine Korrelation zwischen der intraepithelialen T Zelldichte und der Expression von 40 Genen, die an T-Zell-Reaktionen beteiligt sind, (z.B. Granzym A / B, LAG-3, IFN-γ, ZAP70) aufzeigen. Es konnte kein Zusammenhang zwischen Anzahl und Verteilung von T-Zellen mit Plasma-Markern oder dem mGPS gefunden werden.
Schlussfolgerung: Eine Bildanalysemethode zur semi-automatischen, quantitativen und präzisen Beurteilung von T-Zellen getrennt für Tumorepithel und -stroma wurde entwickelt. Die intraepithaliale T-Zelldichte korrelierte mit 40 Genen die an Immunreaktionen beteiligt sind, was darauf hinweist, dass das Tumorepithel gegenüber dem Stroma oder dem vollständigen Tumor, möglicherweise die Region mit dem höheren Potenzial für T-Zell-relevante Biomarker-Forschung ist. Die vorliegenden Ergebnisse können der Ausgangspunkt für Nachfolgestudien sein, die z.B. detailliertere klinische Informationen sowie eine differenzierte Betrachtung von Tumorepithel und -stroma in der mRNA-Expressionsanalyse mittels Laser-Mikrodissektion.

1. INTRODUCTION

1.1 Cancer: A Major Problem In Public Health

Even in the 21st century, cancer remains one of the most important and challenging diseases for mankind and represents one of the leading causes of death, only surpassed by cardiovascular disorders (Hoyert, 2012). Worldwide, an estimated 11 million new cases and 7 million cancer deaths occurred in 2002, while nearly 25 million people were living with cancer (Kamangar et al., 2006). Based on epidemiological data of the SEER program (Surveillance, Epidemiology and End Results) of the National Cancer Institute (NCI) of the United States from 1998 – 2000, the chance to develop cancer during one's lifetime is 50% in males and 33% for females (Gloeckler et al., 2003). In particular colorectal cancer (447.000 cases) and cancers of the lung (410.000) where among the most common cancer types in 2012 and represented the leading cause of cancer related mortality in Europe (215.000 cases and 353.000 cases, respectively) (Ferlay et al., 2013).

1.1.1 Lung Cancer

Various types of benign and malignant tumors can arise in the lung of which 90-95% are carcinomas, being classified into non-small cell lung carcinomas (85%), small cell carcinomas (10-15%) and others types (5%) (Salgia et al., 2010) and representing the leading cause of cancer related death in man and 2nd in women (Ward, 2012; Ferlay et al., 2012). The 5-year survival rate for lung cancer in England between 2005 and 2009 was 7.8 % for men and 9.3 % for woman (Ward, 2012). Among non-small cell lung cancers, adenocarcinomas are the most common histologic subtype in many countries with about 41% of all cases as reported by the NCI SEER Cancer Statistic Review 1975-2010 (Howlader et al., 2010 and 2013). In general, adenocarcinomas are malignant epithelial tumors with glandular differentiation or mucin production. Histologies are defined by the 2004 World Health Organization classification system (Travis et al., 2011) and according to a study on 49 tumors performed by Solis et al. (2012), the most common growth pattern is acinar (Figure 1). They tend to grow more slowly than squamous cell carcinomas, the second major histology of lung cancers, and metastases to distant sites occur early, e.g. before symptoms become apparent or diagnosis (Husain, 2010, Salgia et al., 2010). In resection specimens, they furthermore can be classified in 1. pre-invasive lesions, 2. minimally invasive adenocarcinomas, 3. invasive adenocarcinomas and 4.

variants of invasive adenocarcinomas by addressing primarily their histological features (Travis et al. 2014).

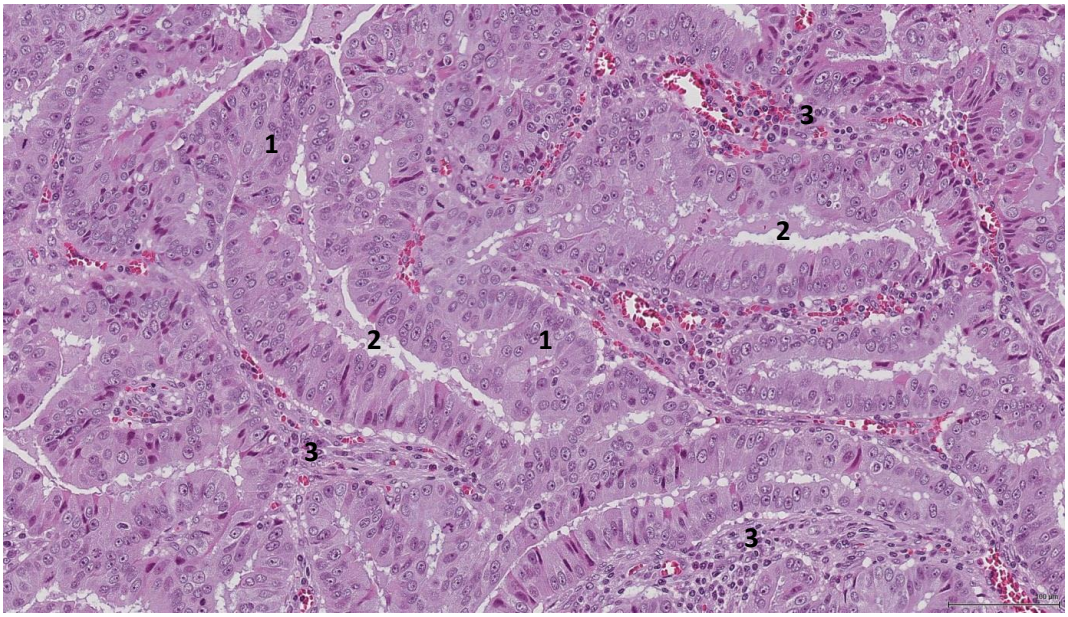

Figure 1 *Histology of a well differentiated adenocarcinoma of the lung. Acinar tumor structures can clearly be recognized: tumor epithelium (1), forming acini with a central lumen (2) and stroma (3). (original magnification 200x)*

1.1.2 Immune System and Cancer

By now, it is well established that immune reactions to malignant tumors do occur and act as an immune surveillance system throughout life. But in the cases, when tumor cells are able to develop effective escape mechanisms, e.g. suppression of immune responses, the immune system turns out to be insufficient to eradicate malignant cells. These escape mechanisms have become a highly interesting target in therapies for cancer since CTLA-4- and PD1-inhibitors have proven to be effective in various cancer types (Hodi et al., 2008 and 2010; Li et al., 2009, Pardoll 2012, Ribas 2010, Topalian et al., 2014). Still, despite the fact that immune-checkpoint therapies are already clinically applied, there is still a lack of pharmaco-dynamic biomarkers to monitor treatment success. Nevertheless, evaluation aspects of immunological responses against malignancies during immunotherapy do likely bear the greatest potential to reveal possible novel biomarkers (Friedman et al., 2011). Promising approaches are the analysis tissue derived markers like number and distribution of TILs and the determination of immune signatures by mRNA-expression analysis. Furthermore, evaluation of plasma based markers, e.g. cytokines, chemokines and other factors involved in inflammatory and immunological responses are of interest as non-invasive methods. With

regards to TIL evaluation, it e.g. could be demonstrated for colorectal cancers (CRC) that the presence of lymphocyte subsets and their location within the tumor is associated with the clinical outcome (Fridmann et al., 2011). Also in NSCLCs, increased infiltration of tumors with adaptive immune cells, particularly CD8+ and CD4+ T-cells in combination with low expression of endothelial growth factors, was shown as an indicator for a favorable prognosis (Broussard, 2011). The distribution of TILs may also provide important information as demonstrated for CRCs: the amendment of the commonly applied TNM-score by an immuno score, as suggested by Galon et al. (2014), improves its prognostic significance. Also, the quantitative evaluation of changes in absolute T-cells numbers correlates with clinical benefit after Ipilimumab treatment in patients with advanced melanoma (Weber et al., 2012). In this context, a technique to quantify not only total T-cells, but also subsets for a better understanding of the mechanisms of immunotherapies would be an important improvement (Ascierto et al., 2013).

1.1.3 T-Lymphocytes: Biology and Subpopulations

The adaptive immune system is largely mediated by T- and B lymphocytes. Immature T lymphocytes are produced in the bone marrow from where they migrate to the thymus for further maturation and differentiation into various lymphocyte subtypes. In order to contribute to immune defense, inactive, naive T lymphocytes must get activated into effector cells, facilitated by cell surface interactions of the CD3/TCR complex with antigen presenting cells (APC) in peripheral lymphatic organs (Anderson et al., 2006). In general, three subtypes of T lymphocytes are crucial for the defense against cancer: CD8+, CD4+ effector and regulatory T-cells (Teff and Treg, respectively). Once activated, cytotoxic (CD8+) T-cells can directly attack and lyse cancer cells (Broere et al., 2011), whereas CD4+ cells play a central role in orchestrating the immune response by down regulating or promoting the activity of CD8+ or other immune cells. Regulatory T-cells are known to down regulate immune responses, helping to avoid unrestricted expansion of activated T lymphocytes and prevent sustained inflammatory responses.

1.1.4 Cytokines: Role in anti-Tumor Immune Responses

Cytokines have an important role in the differentiation, activation and regulation of T-cells. These immune-modulating factors are produced and secreted foremost by T lymphocytes and monocytes, but also by a variety of other cell populations like endothelial cells or fibroblasts (Raphael 2014). They represent a heterogeneous group including chemokines (“chemotactic

cytokines"), interferons, interleukins, lymphokines and tumor necrosis factors. E.g. secreted cytokines can act in an autocrine (affecting the same cell), a paracrine (affecting cells in close proximity) and an endocrine manner (affecting distanT-cells) (Abbas et al., 2012). Their major functions are among others immunomodulation (up- and down regulation), chemotaxis and regulation of inflammatory processes. With regards to their role in cancer, the crosstalk between tumor cells and the microenvironment, including immune-cells, through the release of cytokines can result in the inhibition of tumor development or, in the opposite, in the promotion of growth, invasion and metastasis of cancer (Dranoff, 2004). For example, in cytokine knock-out mouse models, a higher tumor forming incidence was demonstrated (Enzler et al., 2003). However, anti-tumor responses of the immune system depend greatly on the type of involved cytokines, leading to the activation and recruitment of various immune cells such as the Th1 and Th2 cells. Th1 cells are activated through the binding of IL-12, resulting in secretion of the pro-inflammatory cytokine IFN-γ and have been shown to be favorable for tumor suppression. Th2 cells are activated by IL-4, resulting e.g. in the release of IL-4, IL-5 and IL-13 and are rather favorable for tumor survival.

1.1.5 Biomarkers: Definition

According to the NIH's National Cancer Institute (NCI) dictionary of cancer terms biomarkers are termed as *"A biological molecule found in blood, other body fluids, or tissues that is a sign of a normal or abnormal process, or of a condition or disease. A biomarker may be used to see how well the body responds to a treatment for a disease or condition. Biomarkers are also called molecular marker and signature molecules."*

There is no common terminology for the various types of biomarkers. In context of the current study, the following definitions are used as defined by FDA (Tezak et al., 2010) and by the National Cancer Institute Homepage (NCI) Experimental Therapeutics Program (NEXT), respectively:

Predictive markers provide objective information about the likelihood of response (sensitivity or resistance) to a specific therapy.

PD markers are indicators for the pharmacological effect of a drug on its target in an organism.

1.1.6 Role of Plasma Markers in Immunotherapy of Cancer

Assessment of individual cytokine levels in cancer patients provide information about their immune status and have been explored to monitor responses of various tumor types to immunotherapy, such as ovarian, pancreatic and colon cancer (Hanash et al., 2008). Evaluation of the tumor microenvironment through cytokine, gene or protein profiling has greatly expanded our knowledge of cytokine involvement in human disease (Whiteside et al., 2013). Furthermore, cytokines may also serve as predictive factors for better selection of patients likely to respond and/or benefit prior to initiating immunotherapy, including monoclonal antibodies, checkpoint inhibitors, therapeutic vaccines or adoptive T-cell transfer. E.g. Blay et al. (1992) found prognostic significance in metastatic RCC patients, where high pretreatment levels of IL-6 and CRP have been associated with shorter survival upon treatment with IL-2, suggesting that the evaluation of the pretreatment status of particular plasma proteins may distinguish between responder and non-responder of therapeutic treatment. Burgdorf et al. (2009), have shown the importance of changes in pro-inflammatory cytokines (TNF-a, IFN-g and IL-2) upon dendritic cell vaccination in colorectal cancer (CRC) based on vaccination resulting in favorable anticancer responses in terms of polarisation towards a Th1 dominated reactions.

1.2 TNM-Classification

The “TNM Classification of Malignant Tumors”, developed by Pierre Denoix from 1943 – 1952 and maintained by the Union for International Cancer Control (UICC), is a standardized, globally accepted and the most commonly applied staging system for the prognosis of cancer (Wittekind 2010). It describes size and extension of the primary tumor, its lymphatic involvement and the presence of metastases in patients.

1.2.1 TNM: Tumor, Node and Metastases

T: extend of the primary tumor and the presence or absence of invasion into adjacent tissues
N: involvement of local (draining) lymph nodes
M: presence or absence of distant metastasis to distant organs.

The staging of a tumor is done by determining each category: T, N and M

T category: Primary tumor
T0: no evidence for a primary tumor
Tis: cancer cells are growing in the most superficial layer of the tissue, without invasive characteristics into deeper layers.

T1, T2, T3 and T4 describe increasing tumor size and invasiveness into nearby tissue structures.

T1: no larger than 3 cm in greatest dimensions, no invasion of membranes that surround the lungs.

T2: larger than 3 cm but 7 cm or less (T2a: tumor is 5 cm or less; T2b: tumor is larger as 5 cm) or one of the following features:

- involves a main bronchus and is 2 cm or more distal to the carina or
- invasion of the membranes that surround the lungs

T3: more than 7 cm or one of the following features:

- invasion of the chest wall, diaphragm, mediastinal pleura, parietal pericardium or the phrenic nerve.

T4: any size of tumor with invasion of any of the following tissues or organs:

- mediastinum, heart, large blood vessels (e.g. aorta), trachea, esophagus, backbone or carina

N category: Spread of cancer cells to regional lymph nodes

NX: lymph nodes cannot be evaluated

N0: no cancer cells in lymph nodes detected

N1 to 3 N describe the increasing spread of cancer cells into nearby lymph nodes. The higher the number, the more lymph nodes are affected.

N1: spread of cancer into lymph nodes of the lung on the same side as the primary tumor.

N2: spread of cancer into lymph nodes around the carina or the mediastinum on the same side as the primary tumor.

N3: spread of cancer into supraclavicular-, hilar-, or -mediastinal lymph nodes on either side.

M category: distant metastases

MX: no evaluation of metastasis possible

M0: no metastasis in other parts of the body apparent

M1: metastasis apparent

1.2.2 Stage Grouping

For further analyzing it is necessary to combine each classified category (T, N and M) of a tumor into an adequate number of TNM-stage groups, representing a more or less homogeneous group for survival of patients of the same group and a possible distinction of the survival rate for patients grouped into another stage. According to a database of the National Cancer Institute's Surveillance, Epidemiology, and End Results (SEER), the 5-year observed survival rate in patients diagnosed with NSCLC between 1998 and 2000 are 49%, 45%, 30%, 31%, 14%, 5% and 1 % for patients with stage IA, IB, IIA, IIB, IIIA, IIIB and IV.

Stage I: describes a tumor no larger than 3 cm, without invasion of nearby tissues and has not spread into lymph nodes or other parts of the body. Tumor smaller than 3 cm are subdivided into IA (5-year survival: 56%, Vallières et al 2009) and tumors larger than 3 cm but less than 5 cm are staged as IB.

Stage II: describes a tumor either classified as

- Stage IIA: larger than 5 cm but less than 7 cm that has not spread into lymph nodes or a tumor less than 5 cm that has spread into lymph nodes or
- Stage IIB: larger than 5 cm but less than 7 cm that has spread into lymph nodes or larger than 7 cm that has not spread into lymph nodes

Stage III: describes a tumor either classified as

- Stage IIIA: the tumor can show any size (T1-T4) and has spread into lymph nodes but has not spread to distant sides, or the tumor is larger than 7 cm, has spread into lymph nodes and has one or more of the following features:
    - grown either into the chest wall, diaphragm, the mediastinal pleura or the parietal pericardium
    - invasion of the main bronchus or
- Stage IIIB: tumor can show any size, with or without invasion into nearby tissues and has spread into supraclavicular lymph nodes on the same side as the tumor or into hilar-, or -mediastinal lymph nodes on the opposite side and has not spread to distant sides.

Stage IV: describes a tumor that has spread to distant lymph nodes and organs of the body. Cancer cells can also be found in the fluid around the lung or the heart.

1.3 Modified Glasgow Prognostic Score (mGPS)

The modified Glasgow Prognostic Score (mGPS) is based on the assessment of C-reactive protein (CRP) and albumin as serum/plasma markers for inflammation. CRP is upregulated during inflammatory diseases and belongs to the category of "positive acute phase proteins". It represents one of the most commonly applied inflammation markers. Increased levels of CRP are suggested to be predictive for a poor prognosis in prostate cancer (Trautner et al., 1980) and to be associated with shorter survival in several cancer types (e.g. non-Hodgkin's lymphoma, lung-, pancreatic- and oesophageal malignancies) (Mazhar et al., 2006; Proctor et al., 2011; Koch 2009; Martin 2014;). In contrast, albumin, the most abundant plasma protein (55-60 % of total protein) is down regulated under the influence of inflammatory processes and therefore is called a "negative acute phase protein" (Nicholson et al., 2000). The systemic inflammation based prognostic scores are evaluated as follows, indicating a less favorable prognosis at higher stages (Proctor et al., 2013):

- Low-risk of reduced cancer specific survial: (mGPS = 0 points): CRP ≤10 mg/L, albumin ≥35 g/L
- Intermediate-risk (mGPS =1 point): CRP >10 mg/L
- High-risk (mGPS = 2 points): CRP >10 mg/L, albumin <35 g/L

2. AIM OF THE PROJECT

The aim of this exploratory study is to develop a staining technique combined with an image analysis solution to quantitatively investigate the distribution of infiltrating T-cells in adenocarcinomas of the lung with the purpose, to support biomarker discovery for immunotherapies of cancer. Furthermore, distribution and number of the T-cells, determined with the method above, were correlated with gene expression and clinical data (i.e. TNM score) as well as with plasma parameters, to identify possible markers that reflect intra-tumoral immune responses.

The task consisted in the following steps:

- Development of an immunofluorescence staining protocol for FFPE-sections of tumor tissues to detect tumor infiltrating T-cells and to discriminate tumor epithelium from stroma.
- Development of an image analysis solution for the quantification of tumor infiltrating T-cells separately in tumor epithelium and stroma.
- Correlation of number and distribution of tumor infiltrating T-cells with mRNA expression data of relevant genes involved in anti-tumor responses and immune escape of tumors, plasma markers reflecting inflammatory and immunological responses and clinical data (TNM-score).

3. MATERIAL AND METHODS

3.1 Tumor Samples

29 FFPE samples of adenocarcinomas of the lung from different donors were provided by the Indivumed GmbH (Hamburg, Germany).

3.2 Immunohistochemistry

3.2.1 Implementation of an Immunofluorescence Staining Protocol to Visually Separate Tumor Epithelium and Tumor Stroma

Three different staining protocols for elements of the extracellular matrix, collagen type I, collagen type III and vimentin were tested with regards to their suitability to distinguish tumor epithelium and tumor stroma visually. Sections from paraffin-embedded adenocarcinomas with a thickness of 2 µm were prepared on a microtome Hm355 S (MICROM International GmbH, Germany) placed on superfrost microscope slides (Thermo Scientific Superfrost Plus). Slides were incubated at 65°C overnight, deparaffinized in three washings of xylene (247642 Sigma-Aldrich) for 5 min, each, and subsequently rehydrated in ethanol (3x20s ethanol 96%, 3x20s ethanol 70%) and rinsed in distilled water. Two different heat induced antigen retrieval were tested and compared: 1. citrate buffer, 100 mM, pH6, (MERCK, Germany); 2. NaOH buffer, pH9 (Vector Laboratories, # H-3301). In both cases, the slides were treated in an autoclave (MELAG, Melatronic 17 EN) at 121°C/1bar for 20 min. Sections were incubated for one hour at room temperature with the respective primary antibody for collagen type I, collagen type III or vimentin (Collagen type I, host rabbit, LSBio #ID 49771, 1:400 in 2%BSA/PBS. Collagen type III, host rabbit, LSBio #ID 45324; dilution 1:400 in 2% BSA/PBS. Vimentin, host rabbit, Abcam #ab92547, 1:250/1:500 in 2%BSA/PBS), subsequently with the secondary Alexa Fluor 488 labelled antibody (Invitrogen #A11017 dilution 1:1000 in 2% BSA/PBS) for 45 min and counterstained with DAPI. Before mounting with fluorescent mounting medium (Dako #2013-04), the slides were washed 3 times with PBS (SERVA Electrophoresis GmbH, Germany). Evaluation was performed using a Fluorescence Microscope Axioplan-2 from Zeiss.

3.2.2 Double Immunofluorescence Staining of Collagen Type III and CD3

Sections from paraffin-embedded adenocarcinomas with a thickness of 2 µm were prepared on a microtome Hm355 S (MICROM International GmbH, Germany) placed on superfrost microscope slides (Thermo Scientific Superfrost Plus). Slides were incubated at 65°C overnight, deparaffinized in three washings of xylene (247642 Sigma-Aldrich**)** for 5 min, each, and subsequently rehydrated in ethanol (3 x 20 s ethanol 96%, 3 x20 s ethanol 70%) and rinsed in distilled water. Two different heat induced antigen retrieval were tested and compared: 1.citrate buffer, 100 mM, pH6, (MERCK, Germany); 2. NaOH buffer, pH9 (Vector Laboratories, # H-3301). In both cases, the slides were treated in an autoclave (MELAG, Melatronic 17 EN) at 121°C/1bar for 20 min. Sections are incubated for one hour at room temperature with an anti-collagen type III antibody (Collagen type III, host rabbit, LSBio #ID 45324; dilution 1:400 in 2% BSA/PBS) followed by incubation of a secondary anti-rabbit antibody labelled with Alexa Fluor 488 (Invitrogen #A11017 dilution 1:1000 in 2% BSA/PBS) for 45 min at room temperature. This step was repeated accordingly for CD3 antibody (host mouse, Dako #M7254; 1:25 in 2%BSA/PBS; secondary antibody Alexa Fluor 594 (Invitrogen #A11072 dilution 1: 1:1000 in 2% BSA/PBS). The sections were counterstained with DAPI, washed with PBS (SERVA Electrophoresis GmbH, Germany) and mounted with fluorescent mounting medium (Dako #2013-04). The stainings were checked for quality under a fluorescence microscope Axioplan-2 from Zeiss and digitalized for evaluation by image analysis with a Fluorescence Slide Scanner SCN400F® from Leica. The following settings were applied for scanning: exposure time and gain of 100 ms and 8 (blue channel), 130 ms and 7 (green channel) and 130 ms and 7 (red channel).

3.3 Determination of Plasma Markers

3.3.1 Determination of Plasma CRP

The concentration of C-reactive protein in plasma samples from the 29 tumor patients was performed by ELISA (CRP ELISA Kit, IBL Reference number EU59131) according to manufacturer's instructions.

3.3.2 Determination of Plasma Albumin

The concentration of plasma albumin (Albumin, Thermo Fisher Scientific) in plasma samples from the 29 tumor patients was performed on a Konelab™ clinical-chemical analyser (Thermo Scientific™) according to manufacturer's instructions.

3.3.3 Determination of Plasma Chemokines, Cytokines and pro-inflammatory Factors

28 chemokines, cytokines and pro-inflammatory factors were determined in plasma samples of 29 cancer patients using the 30plex Cytokine V-PLEX Human assay from MesoScale Discovery according to manufacturer's instructions, performed on a Discovery Workbench 4.0 (MSD, USA):

Chemokine Panel (#MSD K15047G-1): Eotaxin, MIP-1b, Eotaxin-3, TARC, IP-10, MIP-1a, IL-8, MCP-1, MDC and MCP-4

Cytokine Panel (#K15050D-1): GM-CSF, IL-1α, IL-12/IL-23p40, IL-15, IL-16, IL-5, IL-7, TNF-β and VEGF

Pro-inflammatory Panel (#K15049D-1): IFN-γ, IL-1β, IL-10, IL-12 p70, IL-13, IL-2, IL-4, IL-6, IL-8 and TNF-α

3.4 Gene Expression Analysis

FFPE-sections (60-80 µm) from each tumor were prepared on microtome Hm355 S (MICROM International GmbH, Germany) and deparaffinized in xylene. Purification of total RNA was performed using the RNeasy FFPE Kit (QIAGEN, #73504) according to

manufacturer's instructions and gene expression analysis by using the nCounter GX Human Immunology Kit (GXA-HIM1-48) that includes 581 derived from the Gene Ontology Consortium List of Immunologically Important Genes (GO-LIIG). The nanoString Technology is based on a direct multiplexed measurement of gene expression with high precision and sensitivity. The basic concept behind nanoString is the attachment of a fluorescence colored barcode to a target specific probe corresponding to a certain gene of interest. The binding of a second, also target specific and biotin labeled probe, allows to immobilize the complex by binding to a cell surface in the nCounter Cartridge. Each barcode is finally counted by a digital analyzer (Figure 2). In the current study, a total amount of 150 ng of FFPE-derived total RNA of each sample was used for evaluation. RNA preparation, hybridization, and immobilization was performed according to manufacturer's instructions (The nCounter® Gene Expression Assay Manual). For evaluation and data collection with the nCounter® Analysis System, the samples were submitted to the Uniklinik RWTH Aachen, Germany. Data were analyzed with the nSolver Analysis Software 2.5 (nanoString) with negative background corrections (geometric mean), positive control normalization (geometric mean) and reference gene (n=15) normalization (geometric mean).

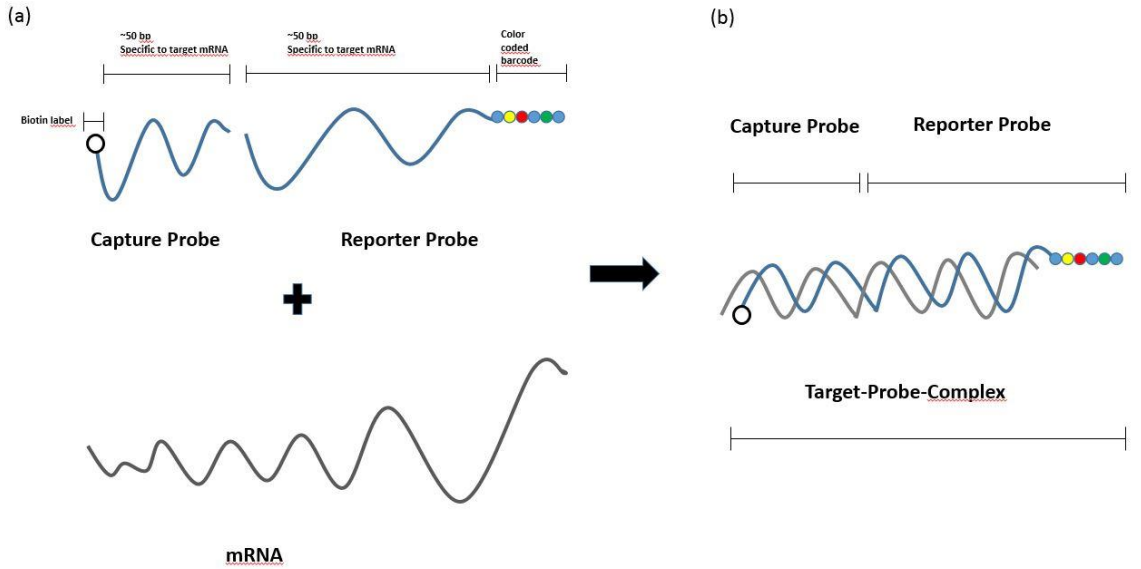

Figure 2 *Main concept of © nanoString Technologies, Inc. (a) shows the composition of the target specific capture probe and the barcoded reporter probe. (b) Each probe binds target specific to 50 nucleotides at the target RNA and forms a complex. The capture probe binds with its biotin-attached end to a cell surface where it gets aligned and immobilized in an nCounter Cartridge.*

3.5 Image Analysis (Definiens Tissue Studio)

For the quantitative evaluation of CD3-positive cells separately for each of the two relevant tumor compartments (tumor epithelium and stroma), a method was developed using the state of the art image analysis software Definiens Tissue Studio (Definiens AG, Germany). The identification of target cells as well as pre-defined regions of interest was performed by machine learning algorithmic settings of multi parametric image features. The image analysis solution was then applied on every digital image for each tumor sample.

3.5.1 Solution: Configuration

General Settings

For an appropriate distinction of tumor epithelium and stroma, the following settings were chosen for the scanned images after upload: magnification (40x), pixel resolution (0.25 µm/pixel) and bit depth (8 bit). Once entered, these parameters were automatically applied after each upload of a slide-scan (Figure 3).

Preselection of Region of Interest (ROI)

Surrounding background (A) was separated manually in each scanned slide, also non-neoplastic lung tissue adjacent to the tumor. The actual tumor tissue was annotated as "ROI"=viable tumor or "No ROI"=areas excluded from evaluation (blood vessels, hemorrhages and necrotic areas), to further increase precision (Figure 3).

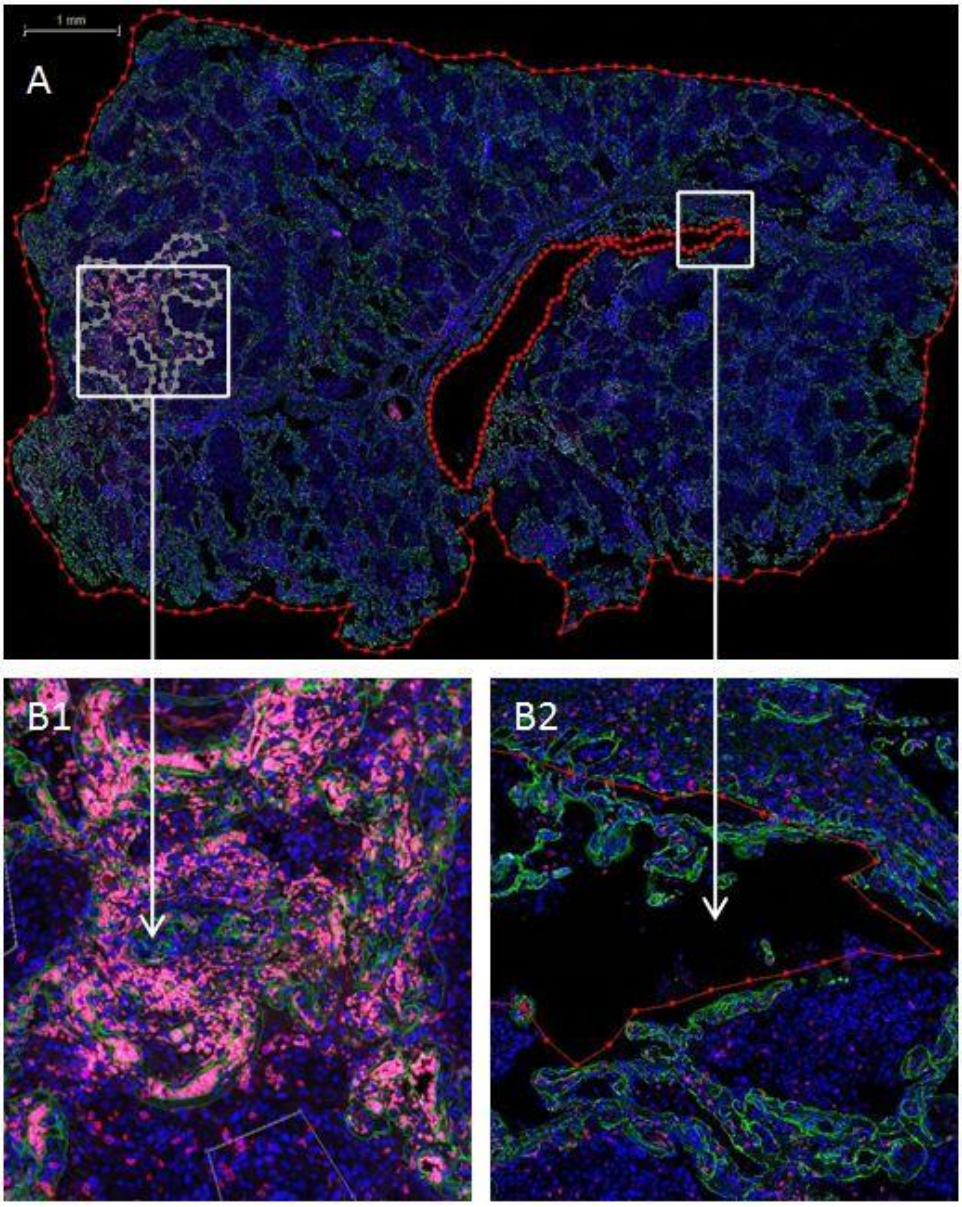

Figure 3 *Preselection of Regions of Interest: Manual separation of surrounding background (black) and viable tumor tissue bordered in red (A, B2). Excluded area: hemorrhages encircled in grey (A, B1).*

Composer – Initialization

The composer technology combines machine learning, pattern recognition and auto-adapted analysis algorithms in order to detect and distinguish ROIs. A 6.4x magnification was chosen to detect differences between ROIs. Out of these predefined image sections within the ROI, a subset of up to twelve images were selected randomly for implementation of evaluation criteria and training of the software (Figure 4).

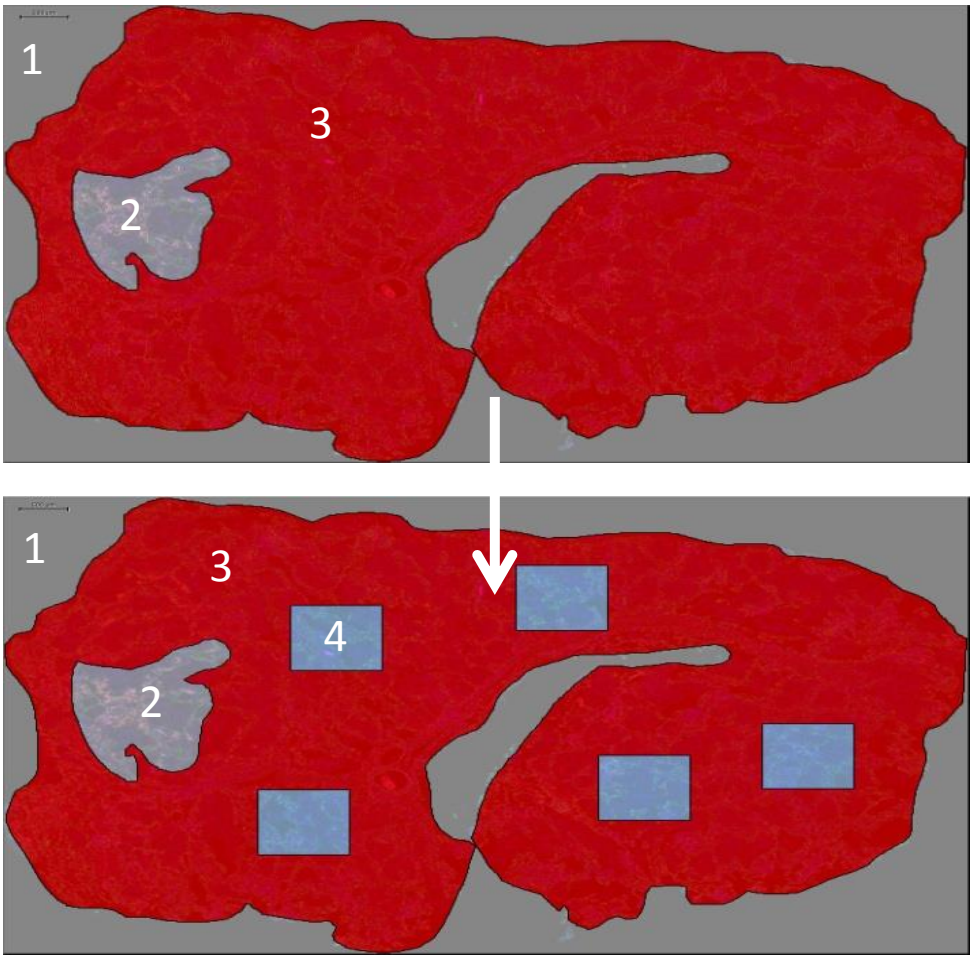

Figure 4 *Randomly selection of images within the predefined image section. (1) deselected area, (2) excluded area: necrosis, (3) ROI, (4) randomly selected examples for composer training.*

Composer – Training

Based on morphological features, substructures are automatically recognized by software specific algorithms and the single images are further pre-segmented at high resolution to facilitate the definition of the ROIs. The resolution of the pre-segmentation then is adapted manually in order to guide the software to distinguish the different relevant structures (tumor epithelium and stroma) with high precision. This is done in the sample selection mode, where segmented objects belonging to the same morphological structure are selected or new segments are defined manually. After completion of the training of Definiens Tissue Studio, the software then is able to categorize the ROIs of the uploaded images into the defined structures. To assure a constant performance of the image analysis across different tumor samples, the automated recognition of structures was controlled by random visual verification before final evaluation. The software discriminates between selected ROIs (Figure 5).

a)

b)

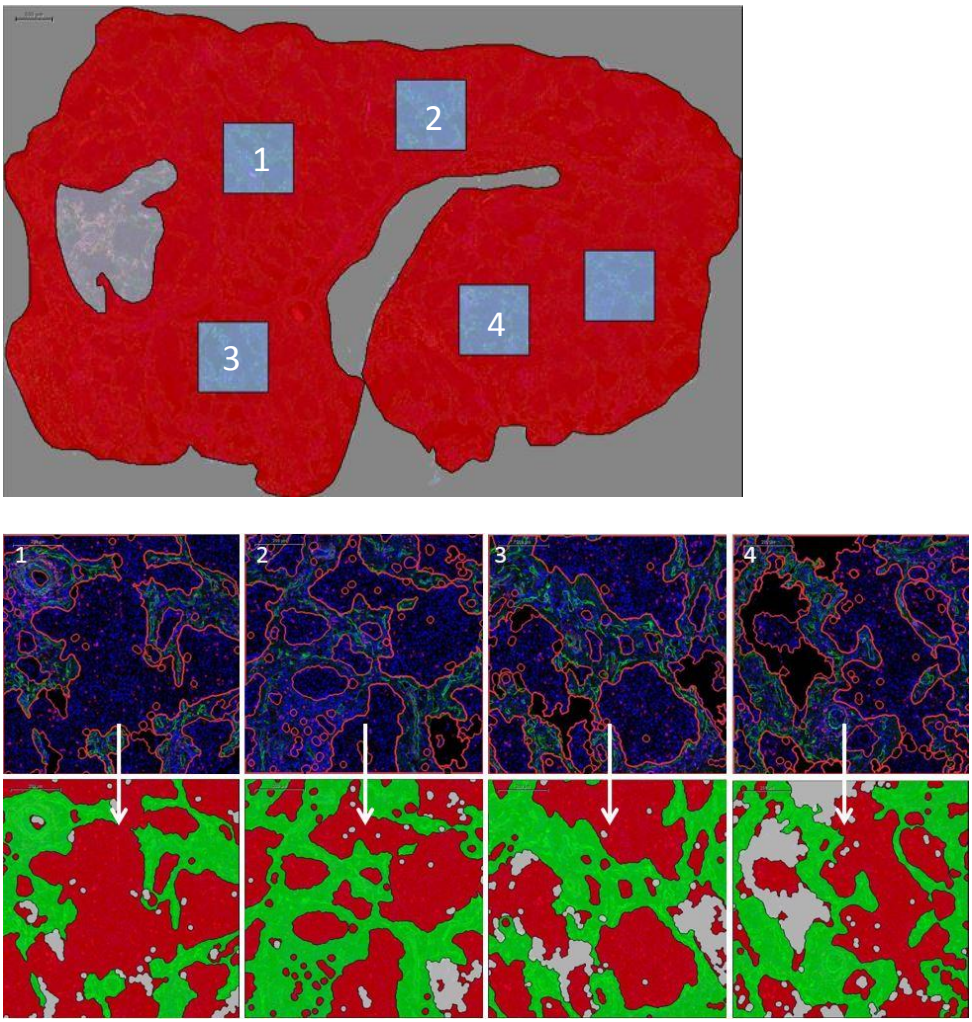

***Figure 5**: ROI classification. (a) Squares 1-4 show randomly selected subsets within the predefined image section (b). Squares 1-4 from (a) shown in more detail and with (b) automated separation of tumor epithelium (red), tumor stroma (green) and blank areas (grey).*

3.5.2 Differentiation between Tumor Epithelium and Tumor Stroma by Immunofluorescence Staining

In order to allow a distinction of tumor epithelium and stroma by the image analysis software Definiens Tissue Studio, immunofluorescence-stainings of two components of the extracellular matrix, collagen type I and III, and vimentin as a marker for mesenchymal cells, were compared. Best results were achieved with immunofluorescence for collagen type III (Figure 6), which exclusively was present in the extracellular matrix. At the same antibody concentration as for collagen type I, a stronger signal was present and a higher percentage of connective tissue could be stained, resulting in a better contrast between tumor epithelium and stroma. Staining for vimentin resulted in a strong signal of stromal cells, e.g. fibroblasts, endothelial cells and leukocytes, but also in staining of leukocytes infiltrating the tumor epithelium. Thus, a distinction between the two compartments was by far less clear than with staining of Collagen type III. Separation process was performed through an automatic segmentation into two compartments: tissue (tumor epithelium and tumor stroma) and background (white space).

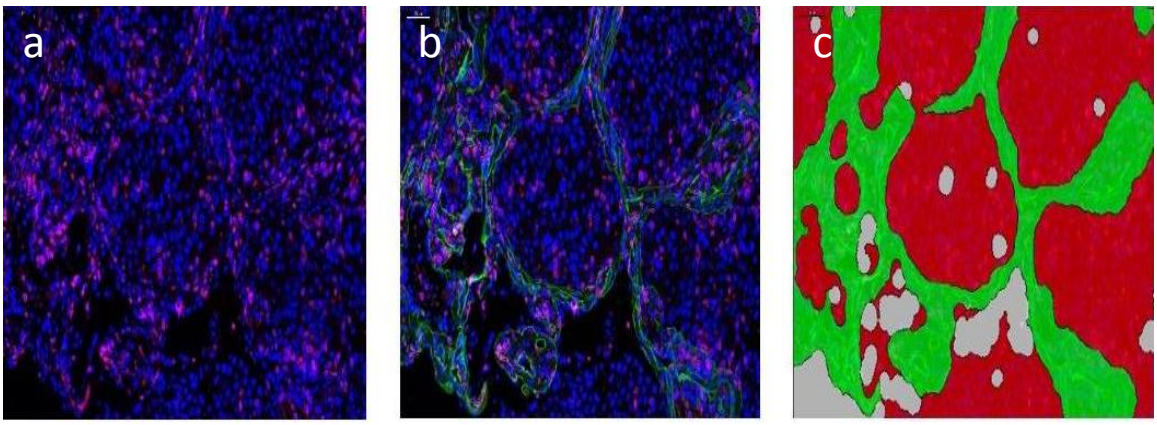

Figure 6 *(a) Immunofluorescence stained section showing CD3+ T-cells (red) and cell nuclei (blue). (b) Additional immunofluorescence staining of collagen type III in the tumor stroma to support (c) automated separation of tumor epithelium (red), tumor stroma (green), and empty areas (white).*

3.5.2 Cellular Analysis

Further subsamples of the uploaded images were chosen randomly for the automated recognition of single cells in the Tissue Studio Cellular Analysis mode. The morphological criterion for cell identification was nuclear staining with DAPI (DAPI channel, blue layer). Furthermore, a membrane mask in the red layer together with staining thresholds detecting membrane autofluorescence at the nucleus region were applied (stain thresholds nucleus region: 0.3/2, membrane stain 60/255) (Figure 7). All cells with a nuclear area more than 60 μm^2 were excluded as artifacts.

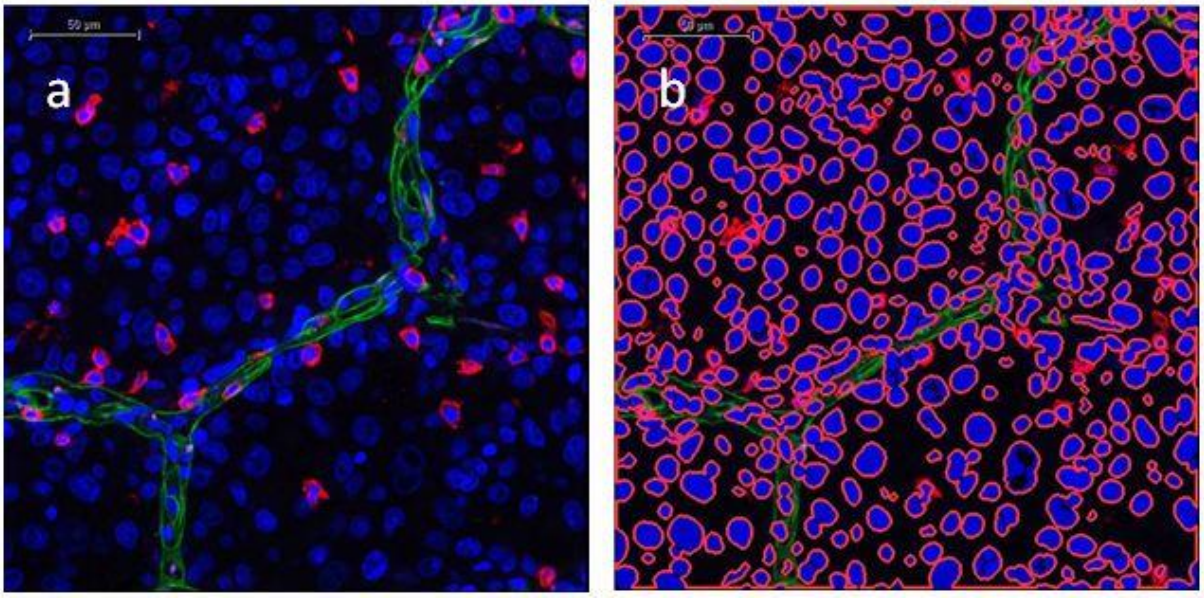

Figure 7 *Cellular analysis (all cells) was performed at the nuclear level. The DAPI channel (blue) as actual nucleus information was used to identify structures as cells within the given threshold. (a) Original scan: immunofluorescence stained section showing collagen type III (green) within the stroma, CD3+ T-cells (red with blue nucleus) and all other cells (blue nucleus without red staining). (b) Automated identification of all cells based on DAPI channel (nuclei).*

3.5.3 Cell Simulation

The Tissue Studio Cell Simulation tool was used to demonstrate the single cells according to the criteria described above and additionally applying criteria for the red and green layer. In this step, CD3+-cells were identified by pixel intensities within a spectrum from 0 (darkest) to 255 (brightest) in the red (<60/255), green (<40/255) and blue layer (0.3/2) and by cell size and shape. The staining intensity in the red channel was used to identify cells being positive for CD3 (secondary antibody labelled with Alexa 594). Background structures showing a signal in the red channel within the threshold for CD3+-cells, like elements of the ECM, were excluded by setting a threshold (>40) in the green layer. Because of their more or less intense green autofluorescence, they could be identified as false positive structures. In contrast, our target cells showed only very little green autofluorescence (<40) and were below this threshhold. Truely positive T-cells were further selected by a defined cellular eliptic fit of 0.6/1 (Figure 8). The elliptic fit measures how closely an object fits into an ellipse of a similar area, e.g.: a perfect circle has an elliptic fit of 1, which is the maximum value.

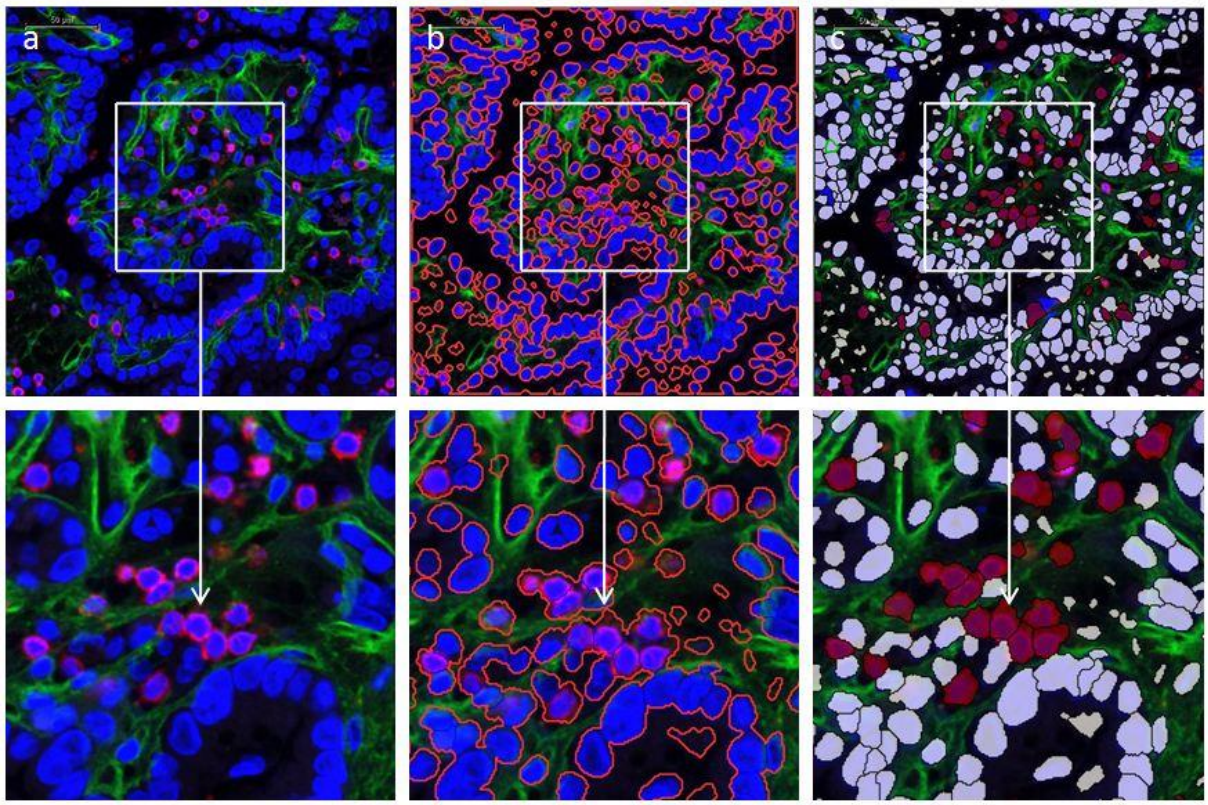

Figure 8 *Cell classification based on size, shape and marker intensity. (a) Immunofluorescence for collagen type III highlighting in green the stroma, nuclei in blue (DAPI) and CD3+ lymphocytes in red. (b) Automated cell classification within the DAPI channel (c) Cells highlighted in red represent detected CD3+ lymphocytes within the red layer. Cells highlighted in white represent detected cells without a signal for CD3.*

3.6 Statistics

Pearson Product-Moment Correlation (PPMC)

Statistical analysis was performed using the software Spotfire 6.5 TIBCO software applying the Pearson Product-Moment Correlation. Number and distribution of T-cells were compared with gene expression data, clinical data (i.e. TNM score) and plasma parameters. Selected cut offs for the p-value was ≤ 0.05 and for the $r^2 \geq 0.5$.

4. RESULTS

4.1 Semi-automated Quantification of CD3+ Fluorescent Labeled Lymphocytes in Tumor Epithelium and Stroma

Automated quantitative assessment of infiltrating T-cells (Table 1) through nucleus detection and cellular analysis was performed with the image analysis software Definiens Tissue Studio. The program was trained to distinguish between red fluorescent membrane labeled target cells (CD3+) and unlabeled nucleus positive cells stained with DAPI, separating tumor epithelium and stroma in adenocarcinomas of the lung with variable morphologies (examples shown in Figures 11-17). Except in four cases, the highest T-cell densities were detected in the tumor stroma (Figure 9). The %-distribution of T-cells between tumor epithelium and stroma was corrected according to the area ratios of these two compartments (Figure 10, formulas see below).

1)

$$\%\ \text{distribution [CD3]} = \frac{[\text{CD3}]_{\text{tumor epithelium, tumor stroma}}}{[\text{CD3}]_{\text{tumor epithelium}} + ([\text{CD3}]_{\text{tumor stroma}} * \text{factor})} * 100$$

2)

$$\text{area (\%)}_{\text{tumor epithelium, tumor stroma}} = \frac{\text{tumor area}_{\text{tumor epithelium, tumor stroma}}}{\text{area}_{\text{tumor epithelium}} + \text{area}_{\text{tumor stroma}}} * 100$$

3)

$$\text{factor} = \frac{\text{area (\%)}_{\text{tumor epithelium}}}{\text{area (\%)}_{\text{tumor stroma}}}$$

Tumor Compartment	T-cells/mm^2				T-cell Distribution/Compartments (mean)
	Mean	**Min**	**Max**	**SD**	
Tumor Epithelium	2470	99	2470	591	30 %
Tumor Stroma	1431	168	2944	802	70 %
Total Tumor	948	207	2409	603	100 %

Table 1 *Mean T-cell densities and distributions (CD3+ cells/mm2) of the evaluated 29 tumor samples.*

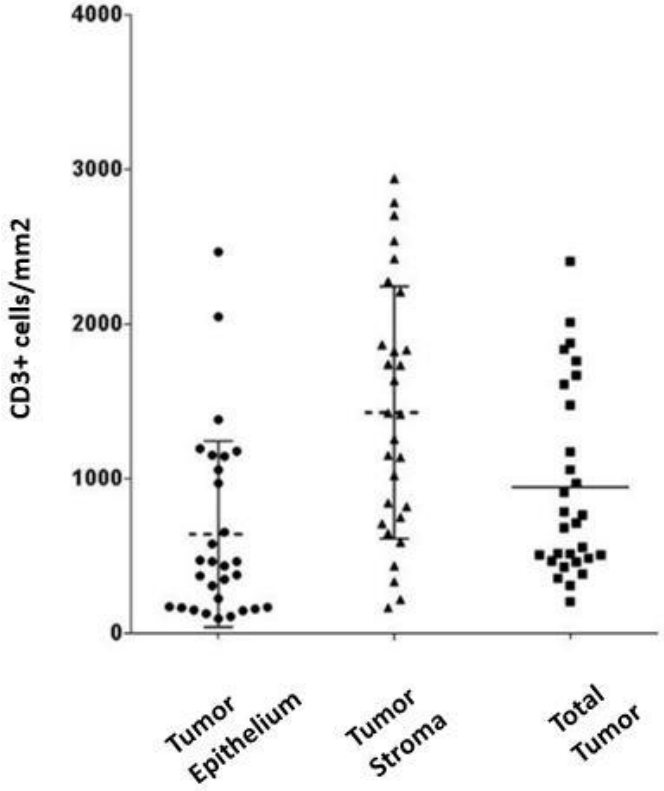

Figure 9 *T-cell densities per tumor (CD3+ cells/mm2): epithelium, stroma and total tumor*

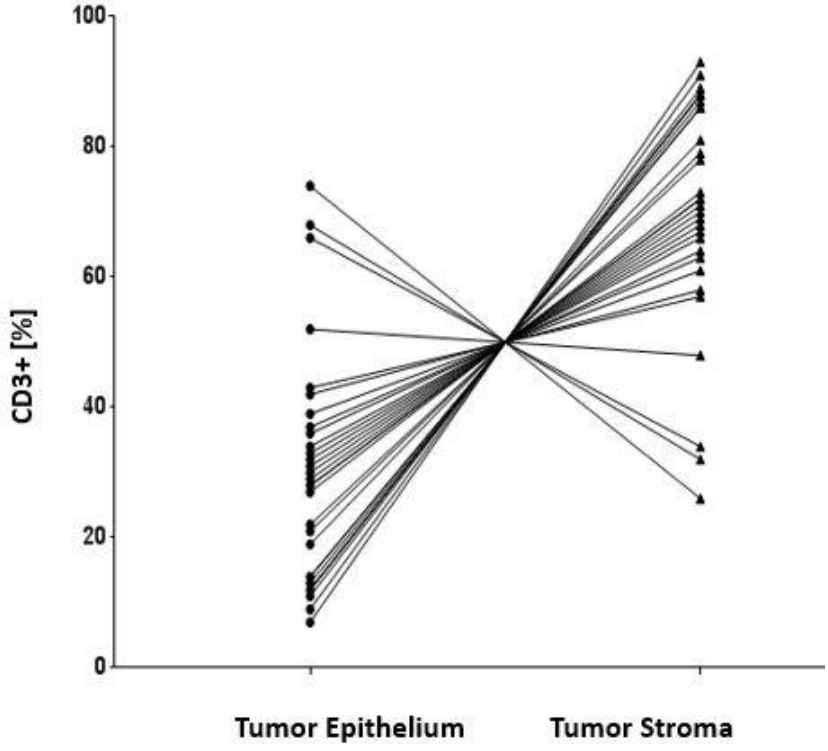

Figure 10 *Distribution of T-cells between tumor epithelium and stroma in % per tumor.*

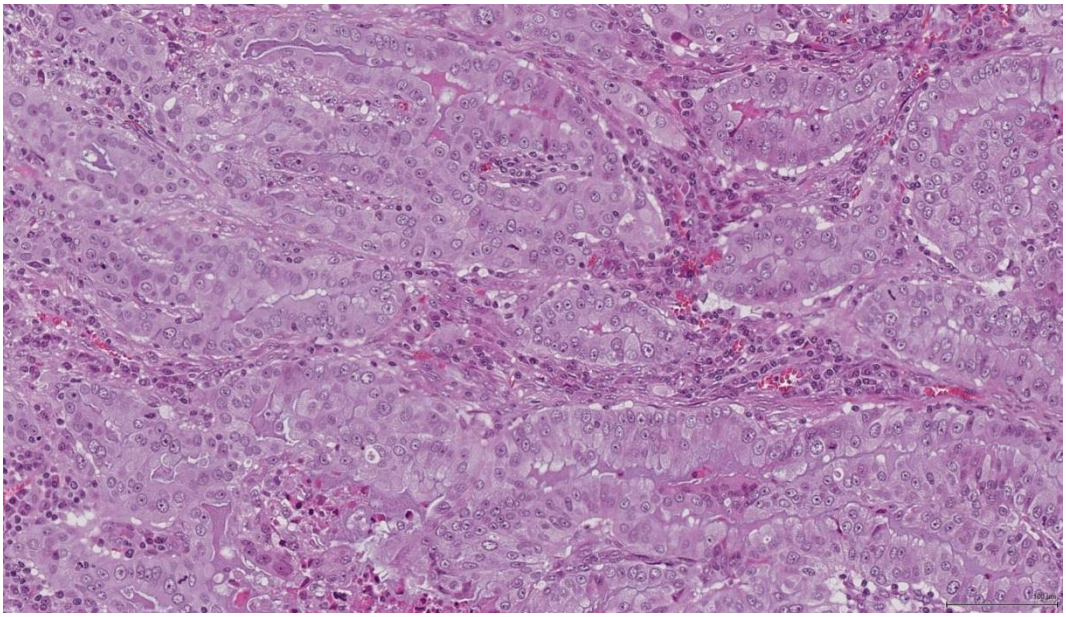

Figure 11 *Well differentiated adenocarcinoma (original magnification 200x).*

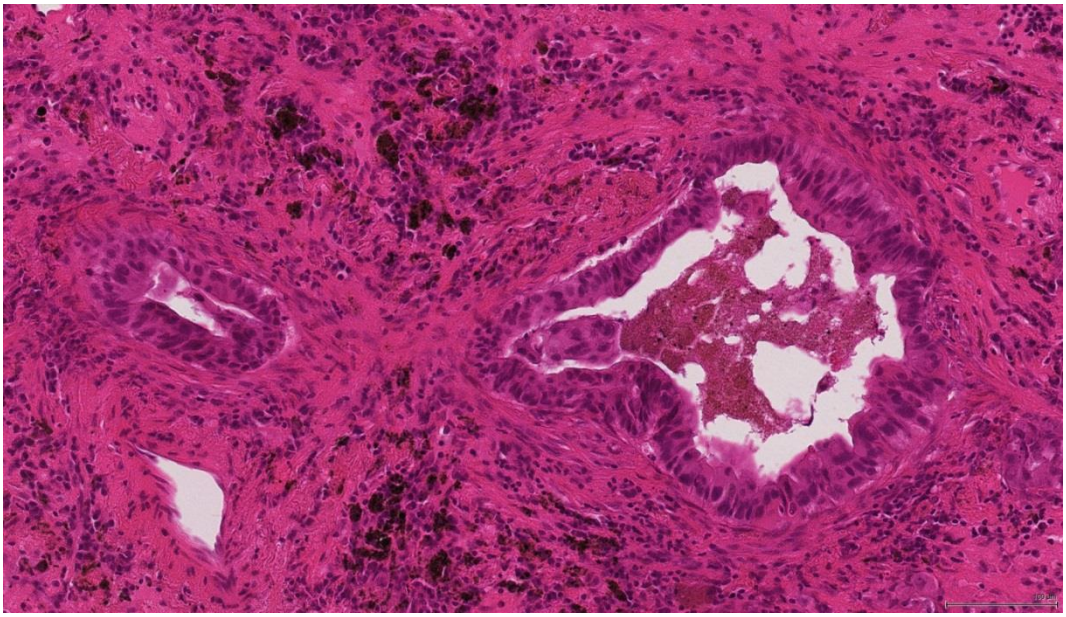

Figure 12 *Poorly differentiated adenocarcinoma with prominent desmoplasia. Many macrophages storing a black pigment, likely coal dust from smoking, are present in the stroma (original magnification 200x).*

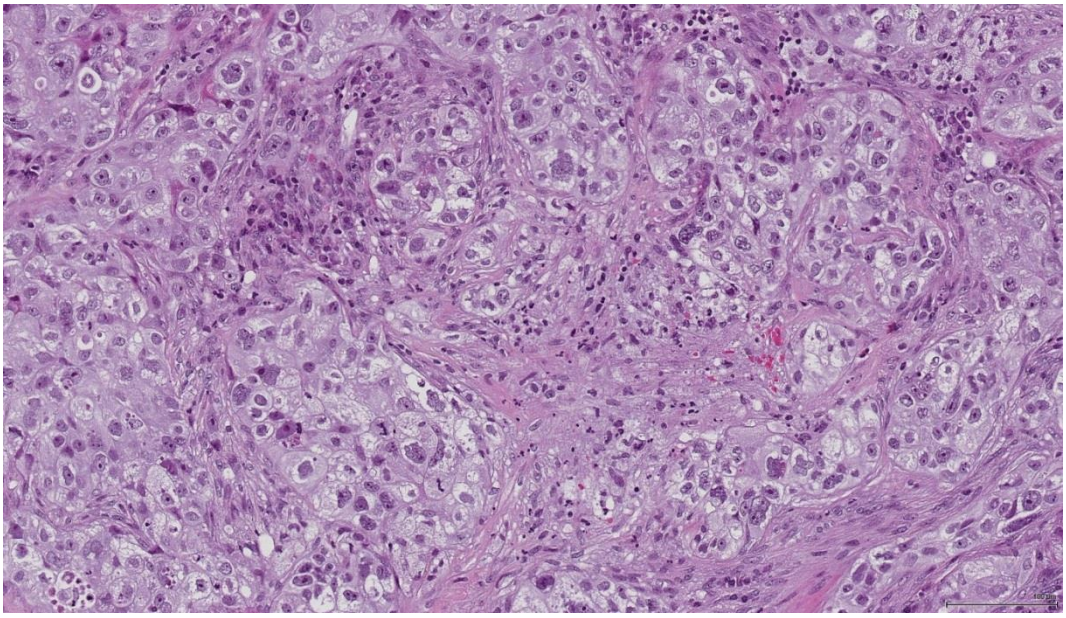

Figure 13 *Poorly differentiated adenocarcinoma (original magnification 200x).*

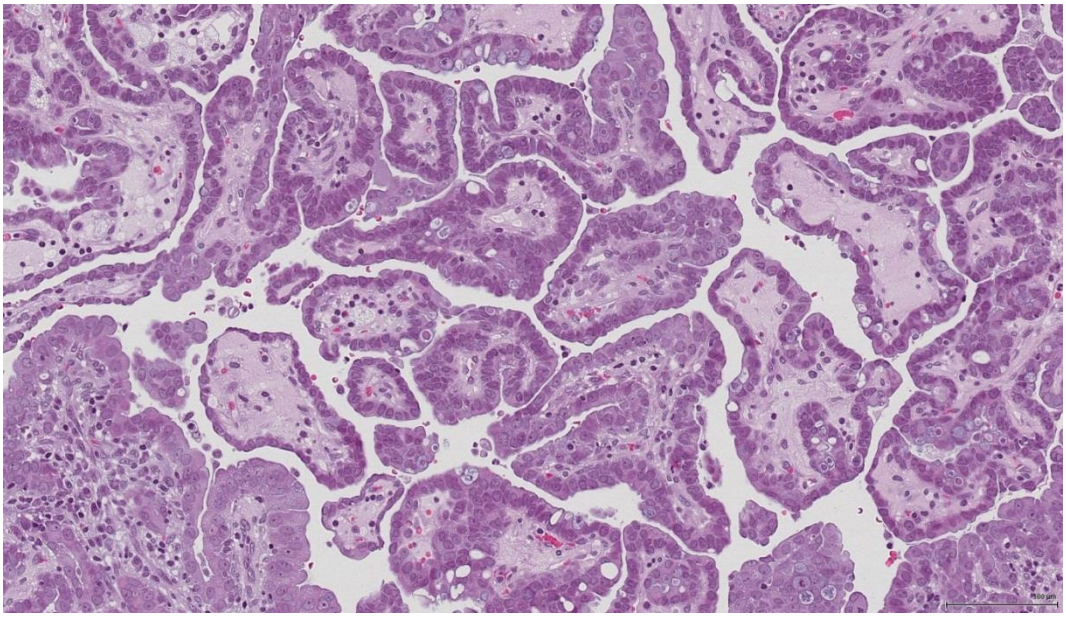

Figure 14 *Adenocarcinoma, papillary pattern (original magnification 200x).*

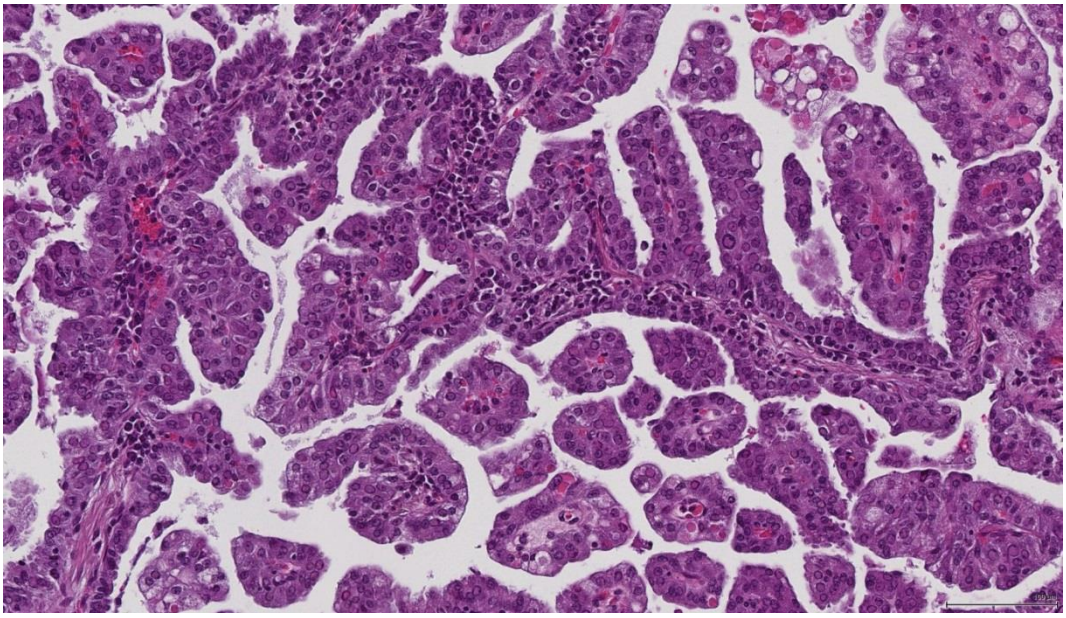

Figure 15 *Adenocarcinoma, micro-papillary pattern (original magnification 200x).*

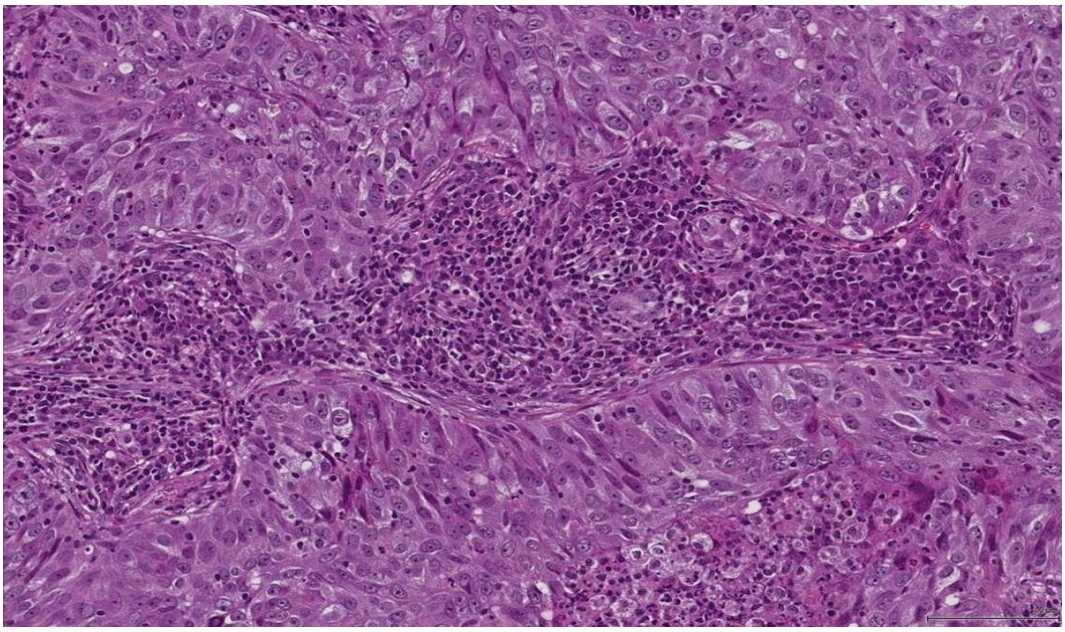

Figure 16 *Moderately differentiated adenocarcinoma, stroma with prominent leukocyte infiltrates (original magnification 200x).*

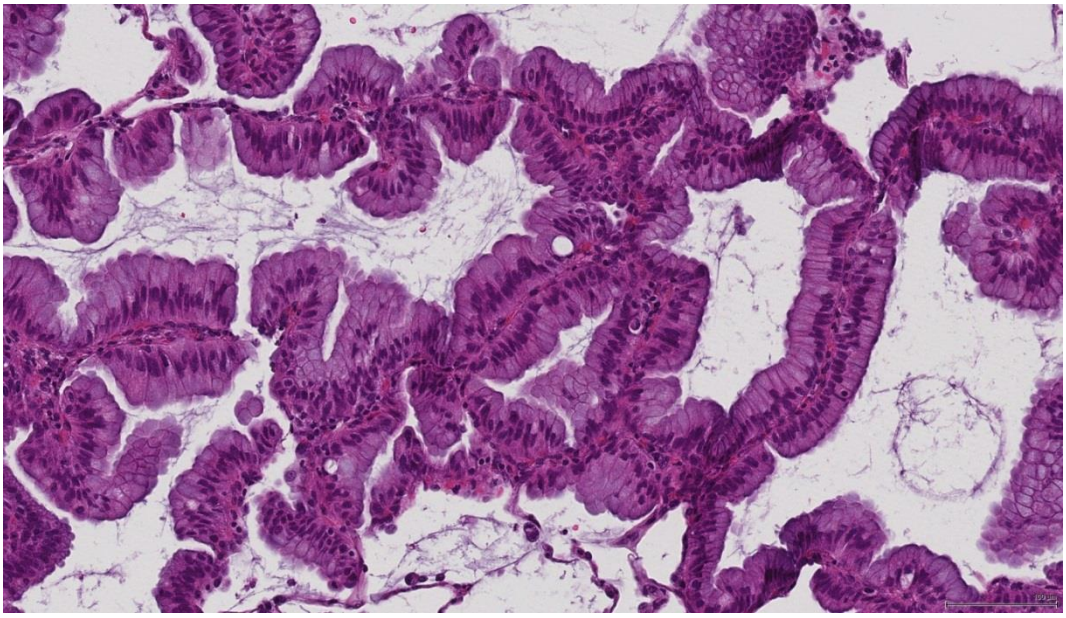

Figure 17 *Broncho-alveolar carcinoma lepidic pattern, mucinous with scant stroma (original magnification 200x).*

4.2 Correlation of Plasma Markers (Cytokines, Chemokines and Pro-inflammatory Factors) with T-Cells (Number and Distribution)

No correlation (in all cases: p-value >0.05, r^2<0.5) was found between number and distribution of infiltrating T-cells between tumor epithelium, stroma and total tumor and determined levels of cytokines, chemokines and pro-inflammatory factors (Table 2; for details see appendix tables 4A-6A).

		Plasma Markers (pg/ml)									
		GM-CSF	**IL-1α**	**IL-5**	**IL-7**	**IL-15**	**IL-16**	**TNF-β**	**VEGF**	**IL-12/IL-23p40**	
Cytokine Panel	**Mean**	0,76	0	236	10	4	1000	0,27	214	2	
	Min	0,28	0	86	1	3	225	0	81	0	
	Max	2	0	653	34	10	2896	0,6	982	31	
	SD	0,32	0	147	6	1	718	0,14	156	5	
		IFN-γ	**IL-1β**	**IL-2**	**IL-4**	**IL-6**	**IL-8**	**IL-10**	**IL-12p70**	**IL-13**	**TNF-α**
Pro-inflam. Panel	**Mean**	44	0,15	0,33	0,06	10	19	0,83	0,94	0,11	4
	Min	4	0	0	0	1	5	0,17	0	0	2
	Max	343	0,47	1	0,23	129	77	2	9	4	11
	SD	80	0,1	0,3	0,06	23	16	0,47	2	0,64	2
		Eotaxin	**Eotaxin-3**	**IL-8**	**IP-10**	**MCP-1**	**MCP-4**	**MIP-1α**	**MIP-1 β**	**MDC**	**TARC**
Chemokine Panel	**Mean**	218	18	0	905	419	122	37	109	1369	275
	Min	107	0	0	301	205	38	15	49	731	30
	Max	418	156	0	3105	902	221	94	344	2865	1059
	SD	69	31	0	568	161	49	16	55	517	208

Table 2 *Plasma concentrations of cytokines/chemokines and pro-inflammatory factors determined in respective plasma samples to the evaluated tumor tissues.*

4.3 Correlation of pTNM Stage with T-Cell Numbers and Distribution

The classification of the 29 tumor samples according to the pTNM-system, as shown in Table 3, was provided by the biobank. No correlation (in all cases: p-value >0.05, r2<0.5) was found between number and distribution (tumor epithelium, stroma and total tumor) of tumor infiltrating T-cells and pTNM-score (Table 3).

pTNM stage	**Tumors (n=29)**
IA	n=3
IB	n=8
IIA	n=6
IIB	n=5
IIIA	n=4
IV	n=3

Table 3 *Numbers of tumor samples per pTNM stage.*

4.4 Correlation of Plasma Markers (CRP, Albumin and mGPS) with T-Cell Numbers and Distribution

No correlation (in all cases: p-value >0.05, r^2<0.5) was found between number and distribution (tumor epithelium, stroma, total tumor) of tumor infiltrating T-cells and determined levels of plasma markers, CRP and albumin as well as for the therefrom derived mGPS (Table 4 and Table 5; for details see Apendix Table 3-A).

	CRP [mg/l]	**ALBUMIN [g/l]**
Mean	20	3
Min	2	3
Max	122	4
SD	30	0,25

Table 4 *Plasma concentration of CRP and Albumin determined in plasma samples matching to the evaluated tumor tissues.*

mGPS	**Tumors (n_{total}=29)**
0	n=0
1	n=15
2	n=14

Table 5 *Number of tumors per mGPS.*

4.5 T-Cell Numbers and Distribution Compared to Gene Expression Analysis (nanoString)

The Pearson Correlation Test indicates a correlation of the mRNA-expression of 49 out of 781 evaluated genes relevant for immune response (p-value <0.00001, r^2 >=0.5) and intra-epithelial T-cell infiltration. 40 of these genes have been described to be expressed in T-cells and to be involved in T-cell reactions (Table 6), whereas 9 genes lacking literature evidence for expression in T-lymphocytes (Table 7, for details see Apendix Table 7-10A).

Th1-Response	CCR5, CXCR3, IFNG, TBX21, STAT1, IRF1
Th17-Response	IL21
Memory T-Cells	CD45/CD45R0, CD86, CXCR3
Activation Markers	CD48, IFNG, LAG3, IL2RB, IL2RG, CD6, CYBB, PDCD1LG2
Effector Molecules	GZMA, GZMB
Pro-inflammatory Factors	CD45RB, CXCR3, C1QB, CD2
Co-inhibtory Receptors	LILRB1, LILRB4
Co-stimulatory Receptors	TLR8, CD244
Chemokine Receptors	CCR1, CCR5, CXCR3
Inhibitory Receptors	IL10A, TIGIT, KLRD1 (as a heterodimer with NKG2-A and NKG2-B molecules)
Inhibitory Molecules	GBP1
Signal Transduction Initiation	CD3D, CD3E, LCP2, ZAP70, GBP5
Apoptosis protection (suggested)	CD53
Transcriptional repressor	GFI1

Table 6 *Correlation of intraepithelial T-cell densities in 29 evaluated adeno-carcinomas of the lung with gene expression analysis: Genes described to be expressed on T-cells and to be involved in T-cell reactions.*

Phagocytosis, Induction of antibody-dependenT-cell-mediated cytotoxicity (ADCC)	FCGR2A/C, FCGR3A/B,
Activation of signal cascades (ERK1, NF-κB)	CMKLR1
Monocyte adhesion and chemotaxis	ITGAX
Receptor for pathogens and damaged cells	CLEC4E
Inhibitory Molecules	CD163
Ligands for Chemokine Receptors	CXCL9, XCL10, CXCL13

Table 7 *Correlation of intraepithelial T-cell densities in 29 evaluated adeno-carcinomas of the lung with gene expression analysis: Genes lacking literature evidence for expression in T lymphocytes.*

5. DISCUSSION:

In the current study, a semi-automated method for the quantitative evaluation of infiltrating T-cells in different compartments of adenocarcinomas of the lung was developed. Based on this technique, T-cell numbers in tumor epithelium, stroma and total tumor were determined and in 29 tumor samples their correlation with the pTNM Score, the modified Glasgow Prognostic Score, the expression of 581 genes involved in immune responses and 29 plasma markers for inflammatory and immunological reactions was analyzed. The microscopical analysis of T-cell infiltrates in tumor sections, e.g. for biomarker research, is time consuming, mostly only semi-quantitative and affected by intra and inter-observer variability (Fuchs 2008). In this study, we focused on the development of a semi-automated and unbiased technique for the detection of the number and distribution of IF stained T-cells as an effective, time saving and precise tool for investigations of this type. The method is based on the image analysis software Definiens Tissue Studio™, a state of the art technology to recognize morphological patterns and different cell types in immuno-histology. This programmed solution combined with double immuno-fluorescence allowed us, to evaluate even morphologically very heterogeneous adenocarcinomas and can likely be adapted to other tumor entities quite easily. Different scoring systems for T-cells infiltrates have been published in the past and have been shown to improve the prediction of disease outcomes in certain tumor entities when combined with TNM staging (Broussard et al., 2011), although no global harmonization has been achieved yet. But even the most advanced of these systems were only able to roughly separate defined tumor areas, like invasive margin and tumor center (Galon et al., 2014), whereas our solution can provide a higher resolution by clearly distinguishing between tumor epithelium and tumor stroma. Collagen type III was selected as marker because of its constant expression within the tumor stroma, whereas epithelial markers may show spatiotemporal changes. E.g. reduced or absent expression of E-Cadherin or cytokeratins in parts of the tumor may negatively influence the accuracy of the achieved results. The significance of infiltrating T-cells in cancer has been studied intensely and meanwhile, there is hard evidence that they may serve as a prognostic biomarker e.g. for CRC and breast cancer (Hadrup et al., 2012 and Azimi et al., 2012) or as predictive and/or pharmcodynamic biomarker for immune-checkpoint therapies like anti-CTLA4 and anti-PD1 treatment (Brahmer et al., 2010). As expected, in our study CD3+ cells were present in all tumor samples and in accordance with prior studies described in literature and based on microscopical scoring, higher T-cell densities were observed in the majority of cases within

the tumor stroma (25 out of 29) when compared to the tumor epithelium (Salmon et al., 2012). The observed selective association of T-cells located in the tumor epithelium with about 10% of the 581 genes of the applied panel relevant for immune responses, points towards that the tumor epithelium might be a more interesting compartment for T-cell evaluation as potential biomarker when compared to stroma or total tumor. The evaluated genes are not exclusively expressed in CD3+ lymphocytes, but our results are suggestive for differences between intra-epithelial and intra-stromal T-cells at the gene expression level. In a potential follow up experiment, separation of epithelium and stroma by laser capture micro dissection could give more detailed information and therefore might likely reveal further genes correlating with compartment specific T-cell densities. We found evidence that T-cells associated with the tumor epithelium show a higher degree of activation than those in the stroma. Expression of genes involved in T-cell activation or in counteracting their inhibition (e.g. CD48, IFNG, TLR8 and IL2RB), of genes for pro-inflammatory, chemokine and co-stimulatory receptors (e.g. CD2, CD244 and CCR1) correlated with intra-epithelial, but not with stromal T-cells. Furthermore, the correlation of the effector molecules Granzyme A and Granzyme B, accepted markers for T-cells with cytolytic potential, with intra-epithelial CD3+-cells, likely the CD8+ subset, is not unexpected. In a probable further step, double immunofluorescence for CD8 and Granzyme A or B to identify cytotoxic CD8+ lymphocytes might even reveal a more significant difference between tumor epithelium on one hand and stroma or total tumor on the other hand. Additionally, the observed association with Nox2 mRNA expression, the phagocyte type NADPH oxidase, could be evidence for higher levels of T-cell based ROS production within the epithelium (Jackson et al., 2004). The correlation of genes promoting Th1 lineage commitment, including besides e.g. IFNG and STAT1 also the chemokine receptors CCR5 and CXCR3, with intra-epithelial T-cells indicates that a Th1 driven immune response has not been entirely silenced in our cases, although it was obviously lacking efficacy in sufficiently eliminating tumor cells.

In addition to the results indicating an increased activation status of T-cells and enhanced T-cell based pro-inflammatory reactions within the tumor epithelium, there were also correlations of genes favoring immune escape and suppression with CD3+ cells, like TIGIT, GBP1, LILRB1 and LILRB4. E.g. TIGIT (T-cell immune-receptor with Ig and ITIM domains), an inhibitory receptor, known to be highly expressed on tumor infiltrating T-cells, has been demonstrated to limit the effector function of chronically stimulated CD8+ T-cells and significant tumor clearance. In the current study, its association with intra-epithelial T-cells might be evidence for a higher down regulation of T-cell function particularly in this

compartment (Johnston et al., 2014). This escape mechanism can be triggered by the tumor itself, since e.g. the ligands for TIGIT, CD155 and CD112, can be expressed on neoplastic epithelial cells (Chauvin et al., 2015, Schramm 2014) and it appears reasonable that primarily intra-epithelial T-cells are affected, not at least because of their closer proximity to the tumor cells compared to stromal T-cells.

The expression of the Th17 promoting cytokine IL-21 and its correlation with intra-epithelial T-cells has to be interpreted cautiously. The meaning of Th17 reactions in immune escape or anti-tumor defense is discussed controversial in the literature. Depending on the stimuli they encounter, Th17 cells can feature either regulatory or inflammatory properties (Bailey et al., 2014).

Several genes known to be expressed by memory T-cells, CD45/CD45R0, CD86 and CXCR3, did correlate with the intra-epithelial fraction of CD3+ lymphocytes. There is lack of literature about a potential association of intra-epithelial memory T-cells with clinical outcome in pulmonary adenocarcinomas. At least for high-grade serous ovarian cancer, CD3+CD8+CD103+ lymphocytes, the second most common subset of CD103+ TILs, have been suggested to be predictive for patient survival (Webb et al., 2013). In my opinion, it could be worthwhile to follow up, if also in NSCLCs this T-cell subset could mediate protective anti-tumor immunity, by applying our method for image analysis on a larger set of samples with known clinical outcome.

Nine genes, so far not published to be expressed in T-cells, but in several other cell types of the immune system, were correlated with intra-epithelial T-cell densities, e.g. CD163, CXCL9, and CLEC4E. An interpretation of this result therefore is difficult. Nevertheless, these data depict the diversity and complexity of the immune signature in cancer.

The results did not reveal a correlation between number and distribution of T-cells with the pTNM-score or the mGPS, but this might be due to the comparatively low sample number of n=29. A more detailed follow up evaluation based on our method that e.g. includes the differentiation and activation status of T-cells might elucidate a context with disease outcome and applied scoring systems.

6. ABBREVIATIONS

ABCF1	ATP-Binding Cassette, Sub-Family F, Member 1
ALAS1	5'-Aminolevulinate Synthase 1
APC	Antigen presenting cells
BSA	Bovine serum albumin
C1QB	Complement Component 1, Q Subcomponent, B Chain
CCR	Chemokine (C-C Motif) Receptor
CD	Cluster of Differentiation
CLEC4E	C-Type Lectin Domain Family 4, Member E
CMKLR1	Chemerin Chemokine-Like Receptor 1
COL1	Collagen type I
COL3	Collagen type III
CRC	colorectal cancers
CRP	C reactive protein
CTLA-4	Cytotoxic T-lymphocyte-associated protein 4
CXCL	Chemokine (C-X-C Motif) Ligand
CXCR	Chemokine (C-X-C Motif) Receptor
CYBB	Cytochrome B-245, Beta Polypeptide
DAPI	4′,6-Diamidin-2-phenylindol
EEF1G	Eukaryotic Translation Elongation Factor 1 Gamma
FCGR	Fc Fragment Gamma Receptor
FDA	FDA Food and Drug Administration
GAPDH	Glyceraldehyde-3-Phosphate Dehydrogenase
GBP	Guanylate Binding Protein
GFI1	Growth Factor Independent 1
G6PD	Glucose-6-Phosphate Dehydrogenase
GUSB	Glucuronidase, Beta
GZMA	Granzyme A
GZMB	Granzyme B
HPRT1	Hypoxanthine Phosphoribosyltransferase 1
IFNG	Interferon gamma
IL	Interleukin

IRF	Interferon Regulatory Factor
ITGAX	Integrin, Alpha X
KLRD1	Killer Cell Lectin-Like Receptor Subfamily D
LAG3	Lymphocyte-Activation Gene 3
LCP2	Lymphocyte Cytosolic Protein
LILRB	Leukocyte Immunoglobulin-Like Receptor, Subfamily B
mGPS	modified Glasgow Prognostic Score
NaOH	Natriumhydroxid
NCI	National Cancer Institute
NSCLC	Non-small cell lung cancer
OAZ1	Ornithine Decarboxylase Antizyme 1
PBS	Phosphatgepufferte Salzlösung
PD	pharmaco-dynamic
PD1	Programmed cell death protein 1
PDCD1LG2	Programmed Cell Death 1 Ligand 2
pH	Potentia hydrogenii
POLR1B	Polymerase (RNA) I Polypeptide B
POLR2A	Polymerase (RNA) II (DNA Directed) Polypeptide A
PPIA	Peptidylprolyl Isomerase A
PPMC	Pearson Product-Moment Correlation
PTPRC	Protein Tyrosine Phosphatase, Receptor Type, C
RPL19	Ribosomal Protein L19
SEER	Surveillance, Epidemiology and End Results
SDHA	Succinate Dehydrogenase Complex, Subunit A
STAT1	Signal Transducer and Activator of Transcription 1
TBP	TATA Box Binding Protein
TBX21	T-Box 21
TCR	T-cell receptor
Th cells	T helper cells
TIGIT	T-cell Immunoreceptor With Ig And ITIM Domains
TILS	Tumor infiltrating Lymphocytes
TLR	Toll like receptor
TNM	Tumor Nodes Metastasis
Treg	Regulatory T-cells

TUBB	Tubulin, Beta Class I
ZAP70	Zeta-Chain (TCR) Associated Protein Kinase

7. REFERENCES

1. Abbas et al., 2012. Cellular and Molecular Immunology, Chapter 1: *Properties and Overview of Immune Responses*, page 8-10. Elsevier (2012).

2. Andersen MH, Schrama D, Straten PT, C Becker JC. *Cytotoxic T-cells*. Journal of Investigative Dermatology 126, 32–41 (2006).

3. Ascierto PA, Kalos M, Schaer DA, Callahan MK, Wolchok JD. *Biomarkers for Immunostimulatory Monoclonal Antibodies in Combination Strategies for Melanoma and Other Tumor Types*. Clinical Cancer Research 19:1009-1020 (2013).

4. Azimi F, Scolyer RA, Rumcheva P, Moncrieff M, Murali R, McCarthy SW, Saw RP, Thompson JF. *Tumor-Infiltrating Lymphocyte Grade is an Independent Predictor of Sentinel Lymph Node Status and Survival in Patients With Cutaneous Melanoma*. Jounal of Clinical Oncology (2012).

5. Bailey SR, Nelson MH, Himes RA, Li Z, Mehrotra S, Paulos CM. *Th17 Cells in Cancer: The Ultimate Identity Crisis*. Front Immunol. 5: 276. (2014).

6. Blay JY, Negrier S, Combaret V, Attali S, Goillot E, Merrouche Y, Mercatello A, Ravault A, Tourani JM, Moskovtchenko JF, et al. *Serum level of interleukin 6 as a prognosis factor in metastatic renal cell carcinoma*. Cancer Res. 52:3317–3322 (1992).

7. Brahmer JR, Drake CG, Wollner I, Powderly JD, Picus J, Sharfman WH, Stankevich E, Pons A, Salay TM, McMiller TL, Gilson MM, Wang C, Selby M, Taube JM, Anders R, Chen L, Korman AJ, Pardoll DM, Lowy I, Topalian SL. *Phase I study of single-agent anti-programmed death-1 (MDX-1106) in refractory solid tumors: Safety, clinical activity, pharmacodynamics, and immunologic correlates.* J Clin Onc. 28 (19): 3167-3175 (2010).

8. Broere F, Apasov S, Sitkovsky M, Van Eden W. *T-cell subsets and T-cell-mediated immunity*. F.P. Nijkamp and M.J. Parnham (eds.). Principles of Immunopharmacology: 3rd revised and extended edition, Springer Basel AG (2011).

9. Broussard EK, Disis ML. *TNM staging in colorectal cancer: T is for T-cell and M is for memory*. J ClinOncol. (2011)

10. Burgdorf SK, Claesson MH, Nielsen HJ, Rosenberg J. *Changes in cytokine and biomarker blood levels in patients with colorectal cancer during dendritic cell-based vaccination*. Acta Oncologica 48:1157-1164 (2009).

11. Chauvin JM, Pagliano O, Fourcade J, Sun Z, Wang H, Sander C, Kirkwood JM, Chen TH, Maurer M, Korman AJ, Zarour HM. *TIGIT and PD-1 impair tumor antigen-specific CD8+ T-cells in melanoma patients.* J Clin Invest. 125(5):2046-2058 (2015).

12. Dranoff G. *Cytokines in cancer pathogenesis and cancer therapy*. Nat Rev Cancer 4, 11-22 (2004).

13. Enzler T, Gillessen S, Manis JP, Ferguson D, Fleming J, Alt FW, Mihm M, Dranoff G. *Deficiencies of GM-CSF and interferon gamma link inflammation and cancer*. J Exp Med 197(9):1213-9 (2003).

14. F. Stephen Hodi, Steven J. O'Day, David F. McDermott, Robert W. Weber, Jeffrey A. Sosman, John B. Haanen, Rene Gonzalez, Caroline Robert, Ph.D., Dirk Schadendorf, Jessica C. Hassel, Wallace Akerley, Alfons J.M. van den Eertwegh, Jose Lutzky, Paul Lorigan, Julia M. Vaubel, Gerald P. Linette, David Hogg, Christian H. Ottensmeier, Celeste Lebbé, Christian Peschel, Ian Quirt, Joseph I. Clark, Jedd D. Wolchok, Jeffrey S. Weber, Jason Tian, Michael J. Yellin, Geoffrey M. Nichol, Axel Hoos, and Walter J. Urba. *Improved survival with ipilimumab in patients with metastatic melanoma.* N. Engl. J. Md. 363, 711-723 (2010).

15. Ferlay J, Soerjomataram I, Ervik M, Dikshit R, Eser S, Mathers C, Rebelo M, Parkin DM, Forman D, Bray, F. *GLOBOCAN 2012 v1.0, Cancer Incidence and Mortality Worldwide: IARC CancerBase No. 11*, Lyon, France: International Agency for Research on Cancer (2013).

16. Ferlay J, Steliarova-Foucher E, Lortet-Tieulent J, Rosso S, Coebergh JW, Comber H, Forman D, Bray F. *Cancer incidence and mortality patterns in Europe: Estimates for 40 countries in 2012.* Eur J Cancer 49(6):1374-403 (2013).

17. Fridman WH, Galon J, Dieu-Nosjean MC, Cremer I, Fisson S, Damotte D, Pagès F, Tartour E, Sautès-Fridman C. *Immune Infiltration in Human Cancer: Prognostic Significance and Disease Control*. Cancer Immunology and Immunotherapy, Current Topics in Microbiology and Immunology 344, Springer Verlag (2011).

18. Fridman WH, Galon J, Pagès F, Tartour E, Sautès-Fridman C, Kroemer G. *Prognostic and predictive impact of intra and peritumoral immune infiltrates*. Cancer Res. 71, 56015605 (2011).

19. Fuchs TJ, Wild PJ, Moch H, Buhmann JM. *Computational Pathology Analysis of Tissue Microarrays Predicts Survival of Renal Clear Cell Carcinoma Patients*. Med Image Comput Comput Assist Interv. 11(Pt 2):1-8 (2008).

20. Galon J, Mlecnik B, Bindea G, Angell HK, Berger A, Lagorce C, Lugli A, Zlobec I, Hartmann A, Bifulco C, Nagtegaal ID, Palmqvist R, Masucci GV, Botti G, Tatangelo F, Delrio P, Maio M, Laghi L, Grizzi F, Asslaber M, D'Arrigo C, Vidal-Vanaclocha F, Zavadova E, Chouchane L, Ohashi PS, Hafezi-Bakhtiari S, Wouters BG, Roehrl M, Nguyen L, Kawakami Y, Hazama S, Okuno K, Ogino S, Gibbs P, Waring P, Sato N, Torigoe T, Itoh K, Patel PS, Shukla SN, Wang Y, Kopetz S, Sinicrope FA, Scripcariu V, Ascierto PA, Marincola FM, Fox BA, Pagès F. *Towards the introduction of the Immunoscore in the classification of malignant tumors*. J Pathol 232(2): 199–209 (2014).

21. Gloeckler Ries LA, Reichman ME, Lewis DR, Hankey BF, Edwards BK. *Cancer Survival and Incidence from the Surveillance, Epidemiology, and End Results (SEER) Program.* The Oncologist 8:541-552 (2003).

22. González-Martín A, Mira E, Mañes S. *CCR5 in cancer immunotherapy: More than an "attractive" receptor for T-cells*. Oncoimmunology 1(1):106-108 (2012).

23. Hadrup S, Donia M, Thor Straten P. E*ffector CD4 and CD8 T-cells and Their Role in the Tumor Microenvironment*. Cancer Microenvironment. Springer (2012).

24. Hanash SM, Pitteri SJ, Faca VM. *Mining the plasma proteome for cancer biomarkers*. Nature 452(7187):571-9 (2008).

25. Helen Ward. *Oxford Handbook of Epidemiology for clinicans*, p.346. Oxford University Press (2012).

26. Hodi F.S, Butler M, Oble DA, Seiden MV, Haluska FG, Kruse A, Macrae S, Nelson M, Canning C, Lowy I, Korman A, Lautz D, Russell S, Jaklitsch MT, Ramaiya N, Chen TC, Neuberg D, Allison JP, Mihm MC, Dranoff G. *Immunologic and clinical effects of antibody blockade of cytotoxic T lymphocyte-associated antigen 4 in previously vaccinated cancer patients.* Proc. Natl Acad. Sci. USA 105, 3005-3010 (2008).

27. Hodi, O'Day, McDermott, Weber, Sosman, Haanen, Gonzalez, Robert, Schadendorf, Hassel, Wallace Akerley, Van den Eertwegh, Lutzky, Lorigan, Vaubel, Linette, Hogg, Ottensmeier, Lebbé, Peschel, Quirt, Clark, Wolchok, Weber, Tian, Yellin,. Nichol, Hoos, Urba. *Improved Survival with Ipilimumab in Patients with Metastatic Melanoma.* N Engl J Med 363:711-723 (2010).

28. Howlader N, Noone AM, Krapcho M, Garshell J, Neyman N, Altekruse SF, Kosary CL, Yu M, Ruhl J, Tatalovich Z, Cho H, Mariotto A, Lewis DR, Chen HS, Feuer EJ, Cronin KA (eds). *SEER Cancer Statistics Review, 1975-2010*, National Cancer Institute (2012).

29. Hoyert DL. *75 years of mortality in the United States, 1935–2010.* NCHS data brief, no 88. Hyattsville, MD: National Center for Health Statistics (2012).

30. Husain A. N. *The lung.* In Robbins and Cotran Pathologic Basis of Disease, 8th ed. (V. Kumar, A. K. Abbas, N. Fausto, C. Aster, eds.), p. 681. Saunders Elsevier, Philadelphia PA; 2010:677–738 (2010)

31. Jackson SH, Devadas S, Kwon J, Pinto LA, Williams MS. *T-cells express a phagocyte-type NADPH oxidase that is activated after T-cell receptor stimulation*. Nature Immunology Volume 5, Number 8 (2004).

32. Jeannin P, Herbault N, Delneste Y, Magistrelli G, Lecoanet-Henchoz S, Caron G, Aubry JP, Bonnefoy JY. *Human effector memory T-cells express CD86: a functional role in naive T-cell priming*. J Immunol. 162(4):2044-8 (1999).

33. Johnston RJ, Comps-Agrar L, Hackney J, Yu X, Huseni M, Yang Y, Park S, Javinal V, Chiu H, Irving B, Eaton DL, Grogan JL. *The Immunoreceptor TIGIT Regulates Antitumor and Antiviral CD8+ T-cell Effector Function*. Cancer Cell Volume 26, Issue 6, p923–9378 (2014).

34. Kamangar F, Dores GM, Anderson WF. *Patterns of Cancer Incidence, Mortality, and Prevalence Across Five Continents: Defining Priorities to Reduce Cancer Disparities in Different Geographic Regions of the World*. J Clin Oncol. 24(14):2137-50 (2006).

35. Koch A, Fohlin H, Sörenson S. *Prognostic significance of C-reactive protein and smoking in patients with advanced non-small cell lung cancer treated with first-line palliative chemotherapy*. Journal of Thoracic Oncology, vol. 4, no. 3, pp. 326–332 (2009).

36. Li B, Van Roey M, Wang C, Chen TH, Korman A, Jooss K. *Anti-programmed death-1 synergizes with granulocyte macrophage colony-stimulating factor-secreting tumor cell immunotherapy providing therapeutic benefit to mice with established tumors*. Clin. Cancer Res. 15, 1623-1634 (2009).

37. Martin HL, Ohara K, Kiberu A, Van Hagen T, Davidson A, Khattak MA. *Prognostic value of systemic inflammation-based markers in advanced pancreatic cancer*. Intern Med J. 44(7):676-82 (2014).

38. Mazhar D, Ngan S. *C-reactive protein and colorectal cancer*. From the Department of Oncology, Medical Day Unit, Chelsea and Westminster Hospital, London, UK. Q J Med 99:555–559 (2006).

39. *NCI Experimental Therapeutics Program (NEXT)* http://next.cancer.gov/developmentResources/pd_biomarker.htm

40. Nicholson JP, Wolmarans MR, Park GR. *The role of albumin in critical illness.* British Journal of Anasthesia 85 (4): 599-610 (2000).

41. Pardoll. *The blockade of immune checkpoints in cancer immunotherapy. Nat Rev Cancer*.12:252–64 (2012).

42. Paine A, Kirchner H, Immenschuh S, Oelke M, Blasczyk R, Eiz-Vesper B. *IL-2 Upregulates CD86 Expression on Human CD4+ and CD8+ T-cells.* The Journal of Immunology vol. 188 no. 4 1620-1629 (2012).

43. Proctor MJ, Horgan PG, Talwar D, Fletcher CD, Morrison DS, McMillan DC. *Optimization of the Systemic Inflammation-Based Glasgow Prognostic Score*. Cancer 119(12):2325-32 (2013).

44. Proctor MJ, Morrison DS, Talwar D, Balmer SM, O'Reilly DS, Foulis AK, Horgan PG, McMillan DC. *An inflammatio-based prognostic score (mGPS) predicts cancer survival independent of tumor site: a Glasgow Inflammation Outcome Study*. Br J Cancer 104:726-734 (2011).

45. Raphael I, Nalawade S, Eagar TN, Forsthuber TG. *T-cell subsets and their signature cytokines in autoimmune and inflammatory diseases*. Elsevier (2014).

46. Ravi Salgia, Ramon Blanco and Arthur T. Skarin. *Atlas of Diagnostic Oncology. Chapter 5: Lung Cancer and Tumors of the Heart and Mediatstinum*. Dana-Farber Cancer Institute. Edited by Arthur T. Skarin. Mosby Elsevier (2010.)

47. Ribas. *Clinical development of the anit-CTLA-4 antibody tremelimumab*. Semin. Oncol. 37, 450-454 (2010).

48. Salmon H, Franciszkiewicz K, Damotte D, Dieu-Nosjean MC, Validire P, Trautmann A, Mami-Chouaib F, Donnadieu E. *Matrix architecture defines the preferential localization and migration of T-cells into the stroma of human lung tumors*. J Clin Invest. 122(3):899-910 (2012).

49. Schramm HM. *Should EMT of Cancer Cells Be Understood as Epithelial-Myeloid Transition?* J Cancer 5(2):125-132 (2014).

50. Solis LM, Behrens C, Raso MG, Lin HY, Kadara H, Yuan P, Galindo H, Tang X, Lee JJ, Kalhor N, Wistuba II, Moran CA. *Histologic patterns and molecular characteristics of lung adenocarcinoma associated with clinical outcome*. Cancer 118:2889–2899 (2012).

51. Tezak Z, Kondratovich MV, Mansfield E. *US FDA and personalized medicine: in vitro diagnostic regulatory perspective*. Personalized Medicine, vol. 7, no. 5, pp. 517-530 (2010).

52. Topalian, Sznol, McDermott, Kluger, Carvajal, Sharfman, Brahmer, Lawrence, Atkins, Powderly, Leming, Lipson, Puzanov, Smith, Taube, Wigginton, Kollia, Gupta, Pardoll, Sosman, Hodi. *Survival, durable tumor remission, and long-term safety in patients with advanced melanoma receiving nivolumab*. J Clin Oncol. 32:1020–1030 (2014).

53. Trautner K, Cooper EH, Haworth S, Ward AM. 1980. *An evaluation of serum protein profiles in the long-term surveillance of prostatic cancer*. Scandinavian Journal of Urology and Nephrology 14(2):143-9 (1980).

54. Travis WD, Brambilla E, Noguchi M, Nicholson AG, Geisinger KR, Yatabe Y, Beer DG, Powell CA, Riely GJ, Van Schil PE, Garg K, Austin JH, Asamura H, Rusch VW, Hirsch FR, Scagliotti G, Mitsudomi T, Huber RM, Ishikawa Y, Jett J, Sanchez-Cespedes M, Sculier JP, Takahashi T, Tsuboi M, Vansteenkiste J, Wistuba I, Yang PC, Aberle D, Brambilla C, Flieder D, Franklin W, Gazdar A, Gould M, Hasleton P, Henderson D, Johnson B, Johnson D, Kerr K, Kuriyama K, Lee JS, Miller VA, Petersen I, Roggli V, Rosell R, Saijo N, Thunnissen E, Tsao M, Yankelewitz D. *International association for the study of lung cancer/american thoracic society/european respiratory society international multidisciplinary classification of lung adenocarcinoma.* J Thorac Oncol. 6(2):244-85 (2011).

55. Travis. *Pathology of Adenocarcinoma, In Lung Cancer, 4th Edition* (Jack A. Roth, WaunKi Hong, Ritsuko U. Komaki, eds.) p. 144. Wiley-Blackwell (2014).

56. Wang H, Kadlecek TA, Au-Yeung BB, Goodfellow HE, Hsu LY, Freedman TS, Weiss A. *ZAP-70: An Essential Kinase in T-cell Signaling*. Cold Spring Harb Perspect Biol. 2(5): a002279 (2010).

57. Webb JR, Milne K, Watson P, deLeeuw RJ, Nelson BH. *Tumor-Infiltrating Lymphocytes Expressing the Tissue Resident Memory Marker CD103 Are Associated with Increased Survival in High-Grade Serous Ovarian Cancer.* Clinical Cancer Research; 20(2) January 15, (2014).

58. Weber JS, Hamid O, Chasalow SD, Wu DY, Parker SM, Galbraith S, Gnjatic S, Berman D. *Ipilimumab increases activated T-cells and enhances humoral immunity in patients with advanced melanoma*. J Immunother. Jan;35(1):89-97 (2012).

59. Whiteside TL. *Immune responses to cancer: are they potential biomarkers of prognosis?* Front. Oncol. 3:107 (2013).

60. Wittekind. *TNM Klassifikation maligner Tumoren, 7. Auflage*. International Union Against Cancer. Wiley-Blackwell Verlag (2010).

8. APPENDIX

Appendix Table 1-A *Correlation of intra-epithelial CD3+ cell densities with gene expression analysis.*

Marker Genes	**CD3+ Cell Density Tumor Epithelium**	
	p-value	**r^2**
C1QB	0,000	0,533
CCR1	0,000	0,645
CCR5	0,000	0,560
CD163	0,000	0,526
CD2	0,000	0,602
CD244	0,000	0,504
CD3D	0,000	0,574
CD3E	0,000	0,557
CD4	0,000	0,540
CD45R0	0,000	0,614
CD45RB	0,000	0,501
CD48	0,000	0,559
CD53	0,000	0,574
CD6	0,000	0,548
CD86	0,000	0,516
CLEC4E	0,000	0,514
CMKLR1	0,000	0,562
CXCL10	0,000	0,543
CXCL13	0,000	0,504
CXCL9	0,000	0,585
CXCR3	0,000	0,641
CYBB	0,000	0,515
FCGR2A/C	0,000	0,524
FCGR3A/B	0,000	0,586

Marker Genes	**CD3+ Cell Density Tumor Epithelium**	
	p-value	**r^2**
GBP1	0,000	0,600
GBP5	0,000	0,676
GFI1	0,000	0,549
GZMA	0,000	0,532
GZMB	0,000	0,687
IFNG	0,000	0,593
IL10RA	0,000	0,502
IL21	0,000	0,534
IL2RB	0,000	0,566
IL2RG	0,000	0,547
IRF1	0,000	0,539
ITGAX	0,000	0,502
KLRD1	0,000	0,512
LAG3	0,000	0,618
LCP2	0,000	0,563
LILRB1	0,000	0,559
LILRB4	0,000	0,540
PDCD1LG2	0,000	0,510
PTPRCall	0,000	0,501
STAT1	0,000	0,578
TBX21	0,000	0,583
TIGIT	0,000	0,543
TLR8	0,000	0,656
ZAP70	0,000	0,535

Appendix Table 2-A *T-cell count per area (mm2) in tumor epithelium, stroma and total tumor.*

Tumor Sample #	CD3+ Cells/Area (mm²)		
	Tumor Epithelium	**Tumor Stroma**	**Tumor Epithelium + Stroma**
1	1148	2279	1839
2	1181	2540	1672
3	161	1023	686
4	172	649	313
4	2050	2788	2409
6	99	1420	510
7	581	2425	972
8	112	821	519
9	2470	1258	1479
10	467	168	358
11	438	1141	768
12	1060	2705	1880
13	1156	1825	1613
14	475	221	387
15	351	593	470
16	1385	1868	1764
17	974	1743	1176
18	1198	2944	2015
19	381	753	517
20	131	846	560
21	467	438	464
22	175	1835	717
23	310	711	432
24	168	1428	789
25	150	1153	510
26	657	1737	1061
27	228	1639	488
28	374	2210	915
29	154	337	207

Appendix Table 3-A *Plasma concentration of CRP and Albumin determined in plasma samples and the therefrom calculated mGPS..*

Tumor Sample #	**Albumin [g/l]**	**CRP [mg/l]**	**mGPS Score (0,1,2)**
1	3	4	0
2	3	3	0
3	3	3	0
4	3	13	2
5	3	2	0
6	3	92	2
7	3	2	0
8	3	3	0
9	3	6	0
10	3	74	2
11	3	2	0
12	3	39	2
13	3	6	0
14	3	2	0
15	3	11	2
16	3	2	0
17	3	2	0
18	3	4	0
19	3	53	2
20	3	12	2
21	3	6	0
22	3	122	2
23	3	21	2
24	3	50	2
25	4	2	0
26	3	14	2
27	3	14	2
28	3	14	2
29	3	12	2

Appendix Table 4-A *Plasma concentration of cytokines determined in plasma samples matching to the evaluated tumor tissues.*

Tumor Sample #	**Cytokine Panel (pg/ml)**								
	GM-CSF	**IL-1α**	**IL-5**	**IL-7**	**IL-12/IL-23p40**	**IL-15**	**IL-16**	**TNF-β**	**VEGF**
1	0,28	0	93,93	5,01	0	3,49	224,88	0,04	170,75
2	0,56	0	342,33	10,9	0,5	2,95	1149,7	0,11	157,99
3	0,71	0	141,66	10,79	3,21	3,59	1341,62	0,33	233,36
4	0,82	0	164,64	9,59	1,22	3,75	960,06	0,26	178,98
5	0,65	0	91,37	5,11	0,99	3,15	894,15	0,31	176,09
6	0,53	0	223,3	8,09	0	4,27	1047,54	0,09	327,59
7	0,55	0	204,56	2,43	0,06	3,66	1470,86	0,6	103,44
8	0,31	0	151,67	4,39	0,08	2,75	244,19	0,29	115,36
9	0,97	0	382,32	6,64	2,58	4,27	1995,3	0,37	182,16
10	1,13	0	652,67	16,5	1,36	8,09	1800,57	0,12	106,64
11	0,95	0	165,16	8,54	1,05	4,11	775,57	0,35	80,91
12	0,66	0	266,78	1,47	0	4,49	586,35	0,33	104
13	0,45	0	167,09	11,47	1,21	3,87	750,17	0,32	206,15
14	0,65	0	170,3	7,11	1,5	3,91	765,4	0	194,37
15	0,91	0	130,49	11,48	1,85	3,13	379,13	0,46	228,62
16	0,59	0	187,24	1,74	1,37	3,86	638,94	0,37	171,73
17	0,34	0	91,65	11,96	1,64	3,15	1014,91	0,39	298,64
18	0,71	0	248,33	9,02	0	3,84	482,37	0,2	286,92
19	1,2	0	335,96	7,13	30,97	9,55	2786,54	0,27	234,87
20	1,39	0	441,76	10,87	1,9	5,71	474,6	0,39	162,1
21	1,67	0	206,56	14,6	0,56	4,71	466,23	0,16	164,53
22	0,75	0	261,83	34	1,71	5,13	1234,63	0,28	981,56
23	0,7	0	184,34	6,71	1,17	2,84	695,59	0,29	278,91
24	1,23	0	157,57	13,13	1,87	5,41	679,2	0,34	335,61
25	1,16	0	640,97	7,76	2,77	4,49	2674,9	0,44	230,53
26	0,69	0	162,61	7,83	0	5,16	535,33	0	103,15
27	0,4	0	138,94	17,51	0,89	4,32	677,94	0,09	236,04
28	0,87	0	148,29	12,72	1,02	4,8	563,45	0,47	199,38
29	0,59	0	504,56	9,18	0,06	6,48	380,1	0,15	117,51

Appendix Table 5-A *Plasma concentration of pro-inflammatory factors determined in plasma samples matching to the evaluated tumor tissues.*

Tumor Sample #	**Pro-inflammatory Panel (pg/ml)**									
	IFN-γ	**IL-1β**	**IL-2**	**IL-4**	**IL-6**	**IL-8**	**IL-10**	**IL-12p70**	**IL-13**	**TNF-α**
1	16,9	0	0,32	0,12	2,44	5,45	1,3	0,64	0	2,53
2	28,03	0,17	0,4	0,11	1,19	9,26	1,02	1,61	0	3,98
3	21,31	0,24	0,29	0,09	1,83	9,2	0,9	0,76	3,61	3,74
4	22,4	0,2	0	0,03	129,15	11,52	0,7	0,85	0	3,26
5	21,21	0,08	0	0	1,88	16,18	0,18	0,91	0	3,44
6	20,33	0	0,4	0,08	19,13	10,86	1,11	0,34	0	5
7	19,65	0,19	0,39	0,09	1,27	6,56	0,69	0,44	0	2,93
8	14,19	0,02	0	0	2,44	8,61	0,73	0,72	0	4,21
9	15,6	0,17	0,45	0,01	4,43	6,78	0,59	0,78	0	4,85
10	19,25	0,24	0,32	0	8,42	8,47	0,93	0,27	0	11,34
11	12,67	0,21	0	0,1	1,83	8,53	0,8	0,6	0	3,28
12	25,21	0,18	0,06	0,14	6,35	21,97	1,19	0,69	0	5,27
13	16,32	0,14	0	0,11	5,12	23,4	0,34	0,51	0	2,12
14	29,02	0	0,69	0,06	2,62	14,76	0,75	0,43	0	2,91
15	18,2	0,23	1,03	0,23	9,31	19,99	0,83	0,77	0	3,22
16	4,47	0	0	0	2,19	10,87	0,38	0,24	0	2,95
17	6,55	0,06	0	0	1,68	14,28	0,33	8,99	0	2,83
18	21,18	0,14	0,29	0,07	3,44	39,82	0,42	0,5	0	3,94
19	26,05	0,17	0,7	0	29,02	77,34	1,12	0,75	0	4,29
20	167,57	0,12	1,13	0,17	8,64	38,51	0,93	1,32	0	8,85
21	17,85	0,23	0,41	0	5,22	16,74	0,65	0,89	0	3,35
22	21,36	0,47	0,24	0	15,18	46,87	0,83	0,69	0	3,66
23	42,54	0,3	0,79	0	8,71	25,12	1,1	0,99	0	4,49
24	14,37	0,15	0	0	7,33	44,75	1,34	0,82	0	4,81
25	15,79	0,16	0,32	0,03	2,66	8,43	0,77	1,11	0	3,96
26	17,93	0,15	0	0	3,33	7,7	0,17	0	0	4,37
27	343,34	0,2	0,33	0,13	6,01	24,46	2,12	0,81	0	5,49
28	314,36	0,25	0,37	0,04	5,48	22,48	2,02	0,55	0	5,56
29	51,06	0	0,36	0,04	13,35	19,71	1,17	0,95	0	5,07

Appendix Table 6-A *Plasma concentration of chemokines determined in plasma samples matching to the evaluated tumor tissues.*

Tumor Sample #	Chemokine Panel (pg/ml)									
	Eotaxin	**MIP-1β**	**Eotaxin-3**	**TARC**	**IP-10**	**MIP-1α**	**IL-8**	**MCP-1**	**MDC**	**MCP-4**
1	310,86	92,65	17,36	203,15	301,1	33,02	0	347,13	1079,64	187,05
2	246,79	150,22	10,95	215,17	1130,21	37,25	0	328,88	943,33	132,19
3	196,4	151,62	7,52	153,03	652,46	37,17	0	312,24	935,38	113,43
4	252,4	76,02	8,17	302,26	399,93	24,58	0	323,26	1447,85	64,31
5	313,78	83,59	10,37	124,29	629,46	23,26	0	505,02	1037,24	165,31
6	144,64	61,75	16,98	683,68	1082,18	42,5	0	741,95	1462,22	103,93
7	240,39	49,3	5,62	144,89	829,35	14,5	0	301,3	814,42	138,04
8	137,67	114,64	3,5	76,89	1026,13	42,5	0	311,9	1293,46	67,85
9	204,23	85,21	21,85	183,13	888,2	48,11	0	415,12	1753,02	140,22
10	239,79	178,09	4,08	114,63	910,05	93,5	0	616,61	1489,96	87,72
11	133,8	81,62	11,7	177,24	872,91	39,77	0	386,6	817,08	131,32
12	106,86	59,05	1,56	30,28	1654,96	15,42	0	204,83	2865,18	37,52
13	168,41	115,27	156,1	409,22	485,66	26,37	0	333,78	1378,51	92,21
14	221,61	62,29	4,27	297,68	737	22,49	0	258,46	1282,08	120,52
15	257,93	80,12	0	180,23	453,46	33,18	0	405,33	1207,7	141,53
16	220,82	60,95	15,01	67,62	470,91	43,64	0	397,11	823,62	76,56
17	207,96	61,43	15,19	308,28	544,43	33,95	0	330,9	1146	149,02
18	335,95	128,52	15,67	331,85	643	24,88	0	424,12	1672,52	221,3
19	209,52	80,06	109,6	1058,7	1010,93	35,92	0	517,38	2501,99	197,45
20	318,62	151,7	7,8	184,8	3104,57	73,2	0	902,15	1407,21	179,13
21	120,85	85,54	9,53	227	645,01	27,4	0	247,75	1069,89	73,71
22	189,82	126,1	19,42	280,51	410,21	44,52	0	544,54	946,32	131,21
23	173,71	71,94	11,33	202,65	1254,4	56,87	0	360,02	1512,46	54,05
24	418,42	344,37	13,6	345,1	923,42	48,52	0	816,09	1204,97	205,95
25	194,93	128,19	11,78	341,9	708,32	37,08	0	440,07	2753,55	139,89
26	236,46	67,43	14,54	184,53	531,63	17,33	0	480,66	1202,38	192,99
27	219,33	132,46	7,34	217,76	1804,32	37,11	0	409,85	1144,44	59,03
28	232,62	115,08	8,95	206,43	1902,86	39,91	0	432,47	1262,1	66,27
29	156,55	155,55	14,52	111,76	1284,01	46,78	0	379,42	730,95	101,24

Appendix Table 7-A *Expression measurements for positive control genes (synthetic constructs) determined in tumor samples (n=29) with nanoString Gene Expression Analysis.*

	Gene Name					
Tumor Sample #	**Positive 1**	**Positive 2**	**Positive 3**	**Positive 4**	**Positive 5**	**Positive 6**
1	21751,12	8256,12	1757,12	449,12	59,12	26,12
2	30086,69	10083,69	2458,69	670,69	72,69	48,69
3	24123,51	9347,51	2224,51	566,51	58,51	39,51
4	24394,52	9337,52	2108,52	543,52	67,52	36,52
5	26283,50	9962,50	2460,50	641,50	86,50	45,50
6	27948,52	10172,52	2394,52	585,52	63,52	26,52
7	18380,33	6130,33	1428,33	432,33	42,33	19,33
8	25420,42	8791,42	2161,42	587,42	63,42	26,42
9	20059,86	6734,86	1615,86	449,86	47,86	35,86
10	22007,59	7559,59	1751,59	575,59	71,59	22,59
11	34414,48	11768,48	2763,48	788,48	106,48	52,48
12	17181,76	6135,76	1519,76	417,76	59,76	26,76
13	31060,86	10504,86	2408,86	708,86	83,86	46,86
14	19429,82	7679,82	1828,82	473,82	57,82	41,82
15	24107,89	8504,89	2096,89	611,89	89,89	21,89
16	22209,99	8691,99	2048,99	566,99	51,99	41,99
17	15080,08	5940,08	1355,08	348,08	36,08	21,08
18	15009,99	5122,99	1184,99	365,99	39,99	29,99
19	29357,33	10157,33	2373,33	671,33	81,33	40,33
20	28328,02	9609,02	2174,02	672,02	87,02	46,02
21	19977,44	7793,44	1865,44	495,44	59,44	33,44
22	23713,86	8639,86	1960,86	523,86	63,86	42,86
23	28412,31	9975,31	2296,31	659,31	61,31	29,31
24	11300,49	4387,49	939,49	305,49	33,49	18,49
25	15789,31	6295,31	1503,31	402,31	49,31	25,31
26	36974,10	13016,10	3125,10	864,10	102,10	49,10
27	25620,41	8899,41	2059,41	624,41	64,41	45,41
28	24912,24	8570,24	1942,24	531,24	81,24	37,24
29	19991,86	7102,86	1538,86	508,86	76,86	24,86

Appendix Table 8-A *Expression measurements for negative control genes (synthetic constructs) determined in tumor samples (n=29) with nanoString Gene Expression Analysis.*

	Gene Name							
Tumor Sample #	**Negative 1**	**Negative 2**	**Negative 3**	**Negative 4**	**Negative 5**	**Negative 6**	**Negative 7**	**Negative 8**
1	1,12	5,12	2,12	1,00	2,12	1,00	1,00	1,00
2	5,69	1,00	1,00	1,00	5,69	6,69	1,00	1,69
3	2,51	1,00	1,00	1,00	2,51	3,51	1,00	3,51
4	8,52	6,52	1,52	1,00	4,52	6,52	1,00	1,00
5	4,50	1,50	1,00	1,00	7,50	10,50	1,00	1,00
6	9,52	4,52	1,00	1,00	1,00	8,52	1,00	1,00
7	10,33	4,33	1,00	1,00	7,33	12,33	1,00	8,33
8	5,42	2,42	1,00	1,00	10,42	19,42	1,00	1,00
9	12,86	1,00	1,00	1,00	1,00	9,86	1,00	3,86
10	1,00	3,59	1,00	1,00	13,59	9,59	1,00	1,00
11	2,48	1,00	1,00	1,00	4,48	9,48	1,00	1,00
12	11,76	1,00	1,00	1,00	7,76	9,76	1,00	1,00
13	3,86	1,00	1,00	1,00	6,86	2,86	1,00	4,86
14	2,82	6,82	1,00	1,00	2,82	8,82	1,00	1,00
15	11,89	13,89	3,89	1,00	15,89	5,89	1,00	1,00
16	9,99	1,00	1,00	1,00	2,99	9,99	1,00	2,99
17	14,08	1,00	1,00	1,00	11,08	8,08	1,00	3,08
18	8,99	3,99	1,00	1,00	1,99	3,99	1,00	4,99
19	4,33	3,33	1,00	1,00	6,33	13,33	1,00	4,33
20	6,02	11,02	1,00	1,00	9,02	11,02	1,00	21,02
21	9,44	1,00	1,00	1,00	1,00	16,44	1,00	1,00
22	5,86	1,86	1,00	1,00	8,86	13,86	1,00	1,00
23	7,31	1,00	1,00	1,00	5,31	4,31	1,00	1,00
24	13,49	1,00	1,00	1,00	4,49	6,49	1,00	14,49
25	15,31	1,31	1,00	1,00	5,31	8,31	1,00	2,31
26	5,10	1,00	2,10	1,00	4,10	9,10	1,00	1,00
27	14,41	1,00	1,00	1,00	5,41	1,00	1,00	7,41
28	10,24	1,24	1,00	1,00	7,24	18,24	1,00	4,24
29	14,41	1,00	1,00	1,00	5,41	1,00	1,00	7,41

Appendix Table 9-A-1 *Expression measurements of 48 positive correlating genes determined in tumor samples (n=29) with nanoString Gene Expression Analysis.*

	Gene Name							
Tumor Sample #	**C1QB**	**CCR1**	**CCR5**	**CD163**	**CD2**	**CD244**	**CD3D**	**CD3E**
1	2565,15	329,72	407,37	1409,79	179,12	92,05	397,96	588,56
2	5549,37	551,76	306,62	4107,28	177,43	65,91	285,64	364,04
3	2679,49	295,55	138,26	959,12	58,39	28,90	124,74	124,74
4	1924,23	92,43	210,70	1644,81	93,91	37,72	156,00	244,71
5	4833,98	244,35	228,94	1725,92	74,77	42,39	150,31	201,18
6	14436,21	648,86	1347,13	4145,88	335,06	123,03	1149,24	832,62
7	9607,38	290,73	433,94	2357,14	277,78	78,75	477,63	479,25
8	1448,90	97,21	103,43	445,23	85,40	8,96	110,26	121,45
9	4375,48	237,84	180,98	1529,78	106,93	93,70	202,14	256,35
10	3610,26	237,06	282,27	1198,37	134,68	64,88	308,86	302,88
11	1005,56	91,90	102,87	683,63	41,60	19,65	63,55	91,90
12	3668,67	326,82	318,79	1583,90	230,50	75,00	526,47	552,55
13	2385,20	212,02	191,52	1089,14	72,97	39,99	310,97	162,11
14	2789,57	564,70	257,41	1090,73	99,06	53,44	223,86	277,53
15	2540,20	260,84	213,74	947,55	106,83	50,06	262,05	207,09
16	2518,44	259,66	183,61	1360,26	114,07	56,49	176,00	236,84
17	2465,01	142,87	168,33	923,19	76,46	41,04	147,30	142,87
18	6209,45	294,66	330,52	1921,18	178,34	117,27	325,68	277,21
19	2804,72	169,14	302,81	1300,05	110,22	50,42	338,87	313,36
20	8686,90	312,10	272,69	2266,54	104,40	55,41	233,28	264,17
21	1088,39	81,14	115,04	335,42	78,31	61,36	123,52	168,73
22	5133,84	166,53	245,67	1001,71	150,70	30,59	272,67	273,60
23	9950,29	729,25	700,90	3779,53	421,52	269,01	1055,87	1062,62
24	13804,23	763,88	1121,80	5150,60	488,79	176,72	794,94	826,00
25	9012,57	485,69	771,67	3513,78	401,06	178,31	764,86	754,16
26	6257,39	272,11	313,89	1008,52	52,75	31,86	293,00	282,56
27	6357,35	317,92	429,51	1976,87	222,45	84,82	484,06	631,61
28	2612,22	194,46	211,47	779,88	178,35	61,09	333,21	385,12
29	1106,68	152,39	160,10	519,01	131,60	55,35	234,04	264,85

Appendix Table 9-A-2 *Expression measurements of 48 positive correlating genes determined in tumor samples (n=29) with nanoString Gene Expression.*

	Gene Name							
Tumor Sample #	**CMKLR1**	**CXCL10**	**CXCL13**	**CXCL9**	**CXCR3**	**CYBB**	**FCGR2A/C**	**FCGR3A/B**
1	468,55	110,88	1781,57	1612,15	188,53	2442,79	2468,68	1421,55
2	716,28	263,56	1729,94	1345,68	145,41	2483,00	3183,07	3264,78
3	210,76	481,11	352,08	3179,62	76,82	898,91	1179,08	2017,14
4	221,05	90,95	170,78	822,78	64,34	853,83	1403,82	728,16
5	403,15	267,48	293,69	1399,08	79,39	2613,94	1406,79	2239,31
6	1228,40	2003,00	1703,34	21605,52	425,52	9166,65	3800,98	7379,98
7	682,33	1432,35	1194,48	7586,28	399,95	5476,17	2523,81	4229,37
8	204,10	53,09	8,34	303,54	50,60	672,07	714,33	728,00
9	289,41	798,52	580,33	1041,83	121,47	1314,23	1308,95	2464,68
10	360,05	695,78	587,41	3194,76	115,41	1553,37	1683,01	1790,04
11	251,95	24,22	53,49	143,12	60,80	743,99	1565,27	515,35
12	572,62	606,73	2035,37	3442,94	195,39	2654,38	1934,04	1667,17
13	273,53	417,93	196,87	1066,86	122,89	1722,02	1103,40	1310,20
14	355,36	378,18	939,09	1694,58	150,05	1807,30	1940,15	1958,94
15	384,66	1148,67	905,27	3488,43	152,13	1702,51	1393,28	2621,74
16	441,10	352,01	220,55	1209,24	121,68	1298,33	1542,78	1655,78
17	284,54	530,26	393,01	2173,91	100,81	1576,22	1352,64	2231,47
18	520,51	948,95	1232,96	6412,04	197,73	3049,47	1382,24	3443,98
19	360,85	435,60	1411,74	3174,95	140,12	1663,25	1583,22	1563,88
20	411,15	416,48	221,56	1307,96	144,88	4510,68	2092,93	3336,95
21	171,55	215,34	3,44	745,10	106,57	653,28	619,38	824,22
22	375,09	892,77	536,17	4121,76	89,25	1933,72	1655,33	3323,82
23	902,01	1629,49	1378,45	9168,82	363,48	5975,47	2926,53	8001,34
24	1540,36	9072,91	5261,52	32849,32	367,51	7116,19	5335,47	12042,74
25	1303,75	2449,62	2797,85	15595,96	334,92	4755,94	2914,58	5648,90
26	371,34	804,83	167,66	2752,92	120,65	2899,16	1912,06	3290,87
27	427,03	476,62	2403,39	3756,09	353,87	3113,84	1942,15	2134,33
28	362,75	345,74	324,26	2021,43	208,78	1658,90	1337,55	2714,26
29	475,11	76,91	328,77	309,52	105,41	1261,49	1132,10	341,10

Appendix Table 9-A-3 *Expression measurements of 48 positive correlating genes determined in tumor samples (n=29) with nanoString Gene Expression Analysis.*

	Gene Name							
Tumor Sample #	**GBP1**	**GBP5**	**GFI1**	**GZMA**	**GZMB**	**IFNG**	**IL10RA**	**IL21**
1	1285,07	372,07	186,18	1075,65	567,38	16,75	1640,39	2,64
2	1683,56	516,42	139,89	372,88	757,14	19,53	1439,53	17,32
3	1025,48	446,70	54,70	513,06	262,37	43,64	489,71	4,32
4	658,68	98,34	89,47	380,73	215,14	2,24	615,80	1,48
5	1257,25	158,02	85,56	296,77	199,64	5,39	760,82	1,54
6	11408,48	750,63	253,08	1793,80	1660,93	281,35	2178,27	128,69
7	2357,95	465,49	137,00	781,04	1128,94	90,88	1469,57	24,54
8	217,15	45,63	38,79	194,16	80,43	1,00	347,66	6,48
9	2262,36	504,95	72,54	824,96	411,07	47,42	380,65	5,10
10	1524,12	288,92	91,47	614,67	330,80	22,33	771,56	9,70
11	250,12	67,21	48,00	91,90	65,38	1,00	486,99	1,00
12	2100,58	228,50	183,35	537,50	367,95	23,83	1329,07	26,84
13	1007,13	171,02	69,40	204,89	120,21	12,36	601,56	1,00
14	1195,40	399,65	109,80	309,74	321,82	30,62	1145,74	1,10
15	1351,00	256,01	97,77	454,72	490,95	60,33	615,98	13,22
16	637,75	133,63	76,05	272,70	156,44	18,46	713,81	1,09
17	1136,81	202,64	37,72	369,77	149,51	28,86	415,15	7,83
18	2485,32	437,15	119,21	685,30	443,94	77,53	1095,32	17,43
19	1679,08	293,14	117,26	654,57	576,30	68,01	790,88	21,40
20	1949,14	295,06	120,38	366,42	286,53	4,29	593,28	10,68
21	595,36	81,14	47,23	284,57	99,50	11,92	503,53	1,41
22	2447,67	375,09	71,56	680,48	360,19	36,18	608,79	1,73
23	6271,05	1726,66	227,17	4326,15	1757,71	332,44	1664,58	26,06
24	8473,91	1319,99	295,04	1504,86	3350,66	349,76	2683,63	53,96
25	5554,55	990,53	286,28	1777,47	830,03	168,58	2114,03	100,49
26	2277,65	47,53	63,20	376,57	104,98	52,75	674,26	1,00
27	2746,83	642,76	124,50	1071,76	445,62	73,66	1418,93	15,39
28	1256,09	344,84	99,58	494,33	146,12	29,76	705,58	10,96
29	388,85	53,81	87,70	206,31	87,70	1,00	733,90	1,00

Appendix Table 9-A-4 *Expression measurements of 48 positive correlating genes determined in tumor samples (n=29) with nanoString Gene Expression Analysis.*

	Gene Name							
Tumor Sample #	**IL2RB**	**IL2RG**	**IRF1**	**ITGAX**	**KLRD1**	**LAG3**	**LCP2**	**LILRB1**
1	894,46	1235,66	1110,94	1181,54	132,06	181,47	1943,94	308,54
2	626,84	1295,99	1404,20	1769,69	80,26	207,25	1791,77	271,29
3	225,51	508,14	1015,65	744,08	46,10	97,71	905,05	180,04
4	262,45	484,22	422,12	326,02	70,25	92,43	731,12	83,56
5	364,60	654,44	663,69	905,74	37,76	184,23	891,86	134,89
6	1463,04	2820,01	1528,06	1545,02	402,91	1101,18	1632,66	340,71
7	738,15	1328,79	1874,92	1181,53	89,26	214,67	1721,20	274,55
8	164,33	278,06	390,54	266,25	13,93	35,69	395,51	40,04
9	568,43	2480,55	1964,83	547,27	84,45	322,47	769,43	59,32
10	387,97	647,91	1101,97	495,67	64,88	175,24	906,52	205,82
11	139,46	286,70	281,22	356,21	11,42	30,62	342,49	80,01
12	622,78	1541,76	1559,82	793,33	89,04	198,40	1404,32	226,49
13	351,97	604,23	778,05	490,13	28,40	99,71	804,79	131,80
14	406,36	893,47	1010,21	733,78	54,78	150,05	1329,59	223,86
15	376,81	763,34	1197,59	551,96	71,20	232,46	902,86	224,00
16	212,94	738,79	914,80	394,38	41,28	103,21	670,35	123,85
17	257,98	686,33	1477,71	513,66	26,65	136,23	680,79	98,60
18	513,73	1035,22	1358,00	1135,06	78,50	265,58	1360,91	255,89
19	478,69	760,10	684,47	398,66	88,23	192,00	861,23	234,22
20	413,28	592,22	970,32	1073,64	37,30	78,84	1426,18	196,00
21	283,15	774,77	1457,10	295,87	27,46	64,19	634,91	92,44
22	473,78	538,96	1785,68	575,27	59,45	181,43	931,88	199,12
23	1675,38	4112,90	3344,93	1414,89	212,32	749,49	2473,04	371,58
24	1401,33	2627,42	3889,01	1867,22	238,84	1642,41	3205,71	797,90
25	848,52	1975,90	2878,59	1842,64	112,17	485,69	2387,36	689,96
26	376,57	736,94	470,58	444,46	73,65	57,98	543,69	78,87
27	867,18	1097,80	1392,89	1100,28	41,42	279,48	1194,51	186,49
28	533,72	928,47	1719,77	1139,72	42,29	169,40	1216,70	118,37
29	251,75	692,31	818,62	455,09	12,99	80,77	900,27	112,34

Appendix Table 9-A-5 *Expression measurements of 48 positive correlating genes determined in tumor samples (n=29) with nanoString Gene Expression Analysis.*

	Gene Name							
Tumor Sample #	**LILRB4**	**PDCD1LG2**	**PTPRC all**	**STAT1**	**TBX21**	**TIGIT**	**TLR8**	**ZAP70**
1	423,84	110,88	5398,28	1715,69	96,76	437,96	70,88	701,50
2	786,95	200,62	4292,79	2246,70	95,72	324,29	126,64	459,00
3	301,70	82,96	1444,51	1551,42	32,58	89,11	47,33	165,30
4	90,95	61,38	1779,35	710,42	73,21	150,09	43,64	238,79
5	417,02	96,35	3145,82	1705,88	54,72	282,89	57,81	236,64
6	1570,47	499,03	10501,00	9782,94	275,69	858,06	267,21	617,76
7	670,19	248,66	4159,79	3130,63	94,93	410,47	259,98	495,43
8	164,33	47,49	970,37	534,72	31,34	49,98	25,12	133,88
9	120,15	88,41	1753,26	3201,23	65,93	179,66	61,97	212,71
10	295,57	96,13	2228,14	2180,28	61,56	183,88	63,55	197,84
11	139,46	27,88	850,99	958,00	30,62	58,06	18,73	93,73
12	504,39	182,35	4280,66	2623,28	121,15	464,26	88,04	409,08
13	372,47	48,01	1283,46	1842,35	25,73	151,41	25,73	133,58
14	355,36	81,62	2370,90	1376,55	57,46	290,95	68,20	282,90
15	733,75	88,71	2147,63	1875,84	74,22	163,61	76,64	246,35
16	433,50	95,60	1797,02	1479,77	97,78	149,93	54,32	227,07
17	295,61	146,19	1486,57	1992,39	58,75	119,62	47,68	131,80
18	758,00	191,91	2588,07	3307,31	105,64	290,78	141,51	292,72
19	411,86	155,07	2869,79	1435,48	77,68	254,44	35,47	253,56
20	380,26	123,58	2776,72	1888,43	76,71	181,09	106,53	232,22
21	98,09	82,55	1298,88	1418,96	78,31	95,27	13,33	171,55
22	502,65	139,53	2104,11	3604,08	67,83	239,15	58,52	170,25
23	672,56	367,53	7291,41	6719,14	236,61	650,97	255,51	1030,23
24	2600,80	1414,64	7709,27	5505,56	311,31	808,25	355,68	675,14
25	1223,01	586,85	6999,04	4716,06	235,70	502,23	224,03	804,74
26	345,23	151,99	4016,83	1959,06	37,09	204,21	68,42	151,99
27	704,76	141,85	4186,33	2754,27	110,86	606,81	76,14	714,68
28	201,62	94,21	3053,52	2153,91	126,43	209,68	62,88	317,99
29	144,69	100,79	2435,29	709,26	46,88	190,91	56,89	296,42

Appendix Table 9-A-6 *Expression measurements of 48 positive correlating genes determined in tumor samples (n=29) with nanoString Gene Expression Analysis.*

	Gene Name							
Tumor Sample #	**CD4**	**CD45R0**	**CD45RB**	**CD48**	**CD53**	**CD6**	**CD86**	**CLEC4E**
1	889,75	1741,57	270,89	873,28	2343,96	176,76	386,19	515,61
2	1429,60	1492,54	243,68	685,36	2556,98	144,31	468,94	760,45
3	409,83	670,35	48,56	225,51	1292,13	60,85	189,87	241,48
4	602,49	700,07	98,34	204,79	1041,60	62,86	138,26	147,13
5	1039,87	1234,12	139,52	350,73	1614,92	113,31	281,35	119,47
6	2579,71	3919,71	247,42	1561,98	4886,55	284,17	679,96	597,97
7	1710,68	2344,19	223,57	578,76	2601,48	195,26	511,61	282,64
8	447,10	452,69	48,74	151,28	613,65	45,63	139,47	25,74
9	593,55	877,86	79,16	228,58	838,19	63,29	184,94	202,14
10	671,18	955,05	102,77	391,30	1419,74	106,76	267,65	112,75
11	347,98	379,08	36,11	155,92	615,95	29,71	103,79	51,66
12	1376,23	2069,48	154,26	784,30	2241,04	202,41	450,22	145,23
13	655,04	678,21	64,95	175,48	1010,70	72,97	196,87	59,60
14	708,28	1234,31	95,04	473,45	1744,23	100,40	243,99	570,07
15	652,82	1002,51	108,04	395,53	1270,67	105,02	224,61	153,94
16	708,37	949,57	78,22	352,01	1033,23	54,32	232,50	30,41
17	605,53	853,46	49,89	173,86	951,97	53,21	189,36	156,15
18	951,86	1263,01	113,40	454,60	1958,01	133,75	338,28	234,56
19	588,62	1083,72	111,10	410,10	1793,40	91,75	243,01	119,01
20	1415,53	1615,77	128,90	287,60	1490,09	105,47	270,56	160,85
21	560,04	547,33	28,87	150,36	548,74	62,77	146,12	45,82
22	852,73	1109,71	103,21	286,64	1175,82	96,70	289,43	299,67
23	1796,85	3043,96	347,29	1188,14	3168,13	291,95	489,00	785,93
24	2294,65	4303,13	287,65	874,81	4724,65	229,96	1268,22	366,03
25	1941,86	3332,85	256,13	993,45	3765,71	301,85	574,21	357,29
26	705,60	1144,31	99,76	444,46	1321,89	115,43	282,56	125,87
27	1514,40	2596,81	208,81	512,58	1608,63	120,78	360,07	396,03
28	1043,94	1341,13	163,13	440,62	1492,40	123,75	145,23	257,12
29	881,01	1140,57	92,32	482,81	1164,45	77,68	213,24	32,24

Appendix Table 10-A-1 *Expression measurements of housekeeping genes determined in tumor samples (n=29) with nanoString Gene Expression Analysis.*

	Gene Name				
Tumor sample #	**ABCF1**	**ALAS1**	**EEF1G**	**G6PD**	**GAPDH**
1	588,20	759,35	32163,90	786,95	28854,61
2	372,45	942,04	21401,46	1200,95	70649,03
3	609,92	1118,90	29782,12	6576,61	30237,03
4	548,59	469,25	20672,17	918,85	38337,50
5	544,20	735,00	21607,07	4649,35	43371,98
6	556,50	689,11	27704,66	2077,44	22508,06
7	721,10	557,57	25210,65	3610,48	23892,37
8	704,96	496,37	44985,95	1510,76	40359,70
9	600,27	696,91	19763,44	1337,11	76149,49
10	541,84	1027,47	15376,31	1990,00	40561,18
11	527,45	761,08	24782,00	1037,68	27876,48
12	668,43	944,17	32155,31	1003,47	14794,05
13	593,26	579,14	32207,05	1108,59	29395,11
14	320,13	964,04	34652,45	5934,66	35123,09
15	561,10	494,57	71385,09	1080,04	31760,97
16	713,03	891,86	51396,30	1705,88	52910,25
17	959,83	600,80	36257,93	1426,29	30609,56
18	582,15	508,34	43849,10	1799,25	38038,66
19	775,73	818,11	29295,64	1217,93	36302,30
20	448,36	679,68	13629,67	3151,25	90821,55
21	670,23	801,61	19108,71	907,56	31305,90
22	442,94	701,77	12437,64	996,09	72899,18
23	515,84	762,92	19302,03	801,83	59297,45
24	517,38	454,95	28806,07	518,26	39494,36
25	843,58	578,37	25177,70	1167,36	50040,11
26	548,39	610,48	24260,98	969,49	51917,36
27	579,00	1073,40	25984,45	4579,85	42891,00
28	1050,30	512,36	36220,36	804,83	38962,30
29	371,23	503,90	20702,71	957,69	25016,23

Appendix Table 10-A-2 *Expression measurements of housekeeping genes determined in tumor samples (n=29) with nanoString Gene Expression Analysis.*

	Gene Name				
Tumor Sample #	**GUSB**	**HPRT1**	**OAZ1**	**POLR1B**	**POLR2A**
1	658,86	669,91	7992,96	238,16	2191,49
2	1094,15	691,23	9320,96	205,77	2579,64
3	917,55	837,38	4953,96	373,76	2076,58
4	1197,87	641,16	3907,37	264,29	2530,80
5	715,06	897,88	7886,92	267,65	2098,51
6	1453,70	401,02	4708,66	231,83	4426,97
7	1124,41	875,60	7799,09	354,91	2160,77
8	516,88	606,01	5395,39	215,59	1985,87
9	687,85	1186,72	5656,66	207,70	1336,50
10	1162,20	947,98	6445,00	188,03	2281,77
11	1359,03	683,20	5310,15	287,55	2345,47
12	1981,64	1039,67	6146,15	232,50	1274,59
13	877,99	590,91	8099,63	306,18	2183,95
14	742,85	946,83	5955,55	156,69	1931,13
15	917,41	609,89	7397,48	308,28	1298,85
16	528,02	1118,49	8017,59	241,27	1832,30
17	821,31	730,84	9163,83	111,73	1994,52
18	541,89	924,33	6789,79	392,94	1279,93
19	1191,85	762,70	6549,25	220,55	2221,83
20	902,16	1018,38	5348,32	155,04	2248,07
21	1602,61	557,22	7095,16	254,90	2150,73
22	928,05	1720,80	10105,25	203,34	1346,61
23	1087,81	1284,30	9926,93	183,17	1434,09
24	642,26	917,51	7309,03	316,00	2245,41
25	1022,51	892,57	6237,20	226,89	1792,57
26	954,65	748,14	7672,02	166,43	3340,89
27	801,52	689,80	5416,89	224,26	2089,21
28	434,02	867,51	5985,81	146,76	2434,33
29	2583,17	857,26	5366,69	159,21	2974,97

Appendix Table 10-A-3 *Expression measurements of housekeeping genes determined in tumor samples (n=29) with nanoString Gene Expression Analysis.*

	Gene Name				
Tumor Sample #	**PPIA**	**RPL19**	**SDHA**	**TBP**	**TUBB**
1	526,36	38868,60	891,85	545,13	4801,82
2	497,85	37829,99	766,47	323,90	3927,58
3	494,95	34101,30	1082,85	544,04	2019,40
4	609,42	33135,36	981,00	753,56	5963,63
5	542,21	35175,65	964,36	496,34	3745,88
6	725,70	32283,92	1986,89	401,02	2898,72
7	586,66	35409,78	837,48	448,21	3278,41
8	867,19	57467,92	880,56	321,66	5618,23
9	530,21	35584,87	695,09	920,98	3740,28
10	348,94	30880,58	825,85	802,58	4825,26
11	795,99	29976,46	1145,09	539,98	2679,35
12	689,23	30532,48	770,10	544,43	3667,62
13	621,50	41433,53	842,69	435,61	4219,38
14	1240,52	45598,88	1169,25	441,78	2620,50
15	503,44	61426,21	929,23	522,66	2327,85
16	259,77	39240,03	861,03	267,48	4289,76
17	507,51	19363,70	1180,34	456,62	8773,70
18	405,01	36582,70	1059,86	588,86	4669,58
19	826,80	34980,07	539,97	484,56	2446,73
20	644,27	29275,91	644,27	1177,76	3942,64
21	585,47	26903,95	911,80	786,07	2892,40
22	570,13	22153,19	546,47	703,24	6030,60
23	417,60	29150,84	591,72	547,94	5628,47
24	390,75	25531,17	924,55	563,99	8563,06
25	319,55	38083,41	657,19	445,23	7193,65
26	476,86	31754,43	749,49	538,94	4639,28
27	521,27	29127,77	1092,02	577,13	3919,71
28	548,92	22729,97	1086,86	392,23	11208,57
29	730,80	46411,52	1215,59	480,34	3375,45

Lebenslauf

Persönliche Daten

Name	Mario Böhm
Geburtstag	27.11.1982
Geburtsort	Wien
Nationalität	Österreich

Ausbildung

April 2014 – März 2015	Masterarbeit am Department für Biomarker und Translation bei Boehringer Ingelheim RCV, Wien Titel der Masterarbeit: "*Integrated T-Cell Analysis of Adenocarcinomas of the Lung: Correlation with Clinical Data and Immune Response Markers*" Betreuer: Prof. Dr. Thomas Decker
2012-2015	Universität Wien – Masterstudium Immunologie
2008-2012	Universität Wien – Bachelorstudium Mikrobiologie und Genetik
2006-2008	Universität Wien – Diplomstudium Biologie
2004-2005	Medizinische Universität Wien
1998-2002	Höhere Lehranstalt für wirtschaftliche Berufe, Baden bei Wien

Curriculum Vitae

Personal information

Name	Mario Böhm
Date of Birth	27.11.1982
Place of Birth	Wien
Nationality	Austria

Education

April 2014 – December 2014	Masterthesis at Boehringer Ingelheim, Vienna Thesis for Master´s degree: "*Integrated T-Cell Analysis of Adenocarcinomas of the Lung: Correlation with Clinical Data and Immune Response Markers "* Supervisor: Prof. Dr. Thomas Decker
2012 – 2015	Studies of Immunology at the University of Vienna
2008-2012	Bachelor in Microbiology and Genetics at the University of Vienna
2006-2008	Studies of Biology at the University of Vienna
2004-2005	Studies of Medicine at the Medical University of Vienna
1998-2002	Higher Federal School for Finance-based Professions in Baden/Vienna